

## Referee #1

Received and published: 12 January 2016

This paper presents the treatment of aerosol background error covariance with balance constraints. Overall, the paper is well written. The presented result shows that the method would improve the chemical data assimilation performance.

We thank Reviewer #1 for thoroughly reviewing the manuscript, valuable comments and constructive suggestions. We have carefully addressed all Reviewer's comments and suggestions. We also respond point by point to the reviewer's comments as listed below.

One major concern is that the numerical experiments were only based on a 24-hour forecasting. Since the atmospheric chemistry and meteorological conditions vary day to day. It is highly suggested that the authors extend the experiments to a longer time period. The test period is coincident with CalNex field campaign. So it is not difficult to find more observations for such testing.

The period of the effect of data assimilation is generally less than 24 hours (Fig. 12). A longer time forecast of the DA experiment should be very close to the experiment without DA. To demonstrate the robustness of our DA system, we conducted nine cases with a group of 24-h forecasts for each case. For the flight events are discontinuous, we ran these cases with different initial time according the flight processes. The details of these nine cases are in Table 2 (Page 19) and Figure 8 (Page 21). And the results are showed in Figure 11 (Page 26) and Figure 12 (Page 28).

Cross-correlations can be between different species/bins or different grid points. The authors often use "cross-correlation" without specifying what they mean. It is helpful to be unambiguous. For instance, in abstract (line 7 on Page 10054), "cross-correlation" probably refers to the correlation between different species.

Thanks, the specification for cross-correlation has been revised in this sentence and some other sentences (line 40, line 123, line 141, line 191, line 268, line 269 and line 580).

The description of model configuration is lacking. Although readers are referred to Li et al. (2013) for details, some basic information should be provided directly. For instance, the mapping projection used for the horizontal coordinates and the extensions of the vertical levels are better given in the paper.

We have added some description of the model configuration in the revised manuscript (lines 273-277).

The calculation of the cross-correlation of emission species is not clear. Is it based on 15 May-14 June, 2010 emissions over domain d03?

The emission species are referred to those RADM2 species that produced by NEI'05 data. We calculated the correlation between any two horizontal fields of emission species over domain d03. It is indicated at line 294.

10054, line 14, "are more coincident" -> have better agreement

Thanks, the sentence has been revised (line 47-49).

10054, line 23, "meteorology-chemistry models" -> Chemical transport models

The "meteorology-chemistry models" has been revised as "Chemical transport models" (lines 62).

10055, line 4, "difficult dealt due to ...": Remove "dealt".

The "dealt" has been removed.

10055, line 26, "balance analysis fields": balanced analysis fields?

Corrected.

10056, line 16: PM2.5 is part of PM10 and PM1 is part of PM2.5. So they do not represent different size bins.

This sentence has been revised, and we cited two new papers about the relationship of PM2.5 and PM10-2.5 (lines 109-111).

10056, line 19: The spread of observation impact is not necessarily "enhanced".

Corrected. We have changed to "produce more balanced initial fields" (line 109).

10057, line 4: It is not clear what "the species that are not ADJACENT" means here.

"that are not ADJACENT" means that are not the connecting. This sentence has been revised (line 121-122).

10057, line 12, "... has been ESTIMATED ...": Developed or applied?

The "estimated" has been changed to "developed" in the revised manuscript.

10058, Eq(1): It is better to have the LHS written as  $J(x)$  and  $x$  should be in bold font.

" $J(\delta x)$ " has been changed to " $J(\mathbf{x})$ ", and  $\mathbf{x}$  is in bold font in the revised manuscript.

10059, line 2, " $d = y - Hx$ ":  $d = y - H \mathbf{x}^b$

Corrected.

10059, lines 6-7: This seems to neglect the fact that there are multiple variables at each grid point.

Corrected. The sentence has been change to: For a high-resolution model, the number of vector  $\mathbf{x}^b$  is on the order of  $10^7$ . Therefore, the number of elements in  $\mathbf{B}$  is approximately  $10^{14}$  (line 174).

10059, line 18, “which represent ...”: Separate the run-together sentence. They represent the correlation among pairs of grid points for one species.

Thanks. The sentence has been separated (lines 185-186).

10063, line 16, “cross-correlations between emissions”: Change to “cross-correlations of emission species”, to be consistent with the title of Section 3.2.

The sentence has been revised (Line 265).

10063, line 19, “the cross-correlations of aerosol emissions from ...” -> the cross-correlations of aerosol emission species from ...

The sentence has been revised (Line 268).

10064, line 3, “...that is coupled to aerosol and chemistry domains” -> ...that is coupled to aerosol and chemistry models

The sentence has been revised (Line 272).

10064, lines 16-17, “Emission files are .... of the aerosol forecasts”: What does “a primary factor for the distribution of the aerosol forecasts” mean? In addition, it is a run-together sentence that needs to be rewritten.

“A primary factor” means the emission file. This sentence has been revised as: The emission files are necessary for running the WRF/Chem model. It is an important factor for the distribution of the aerosol forecasts. (lines 290-291)

10065, line 5: “With the exception of the auto-correlation in the diagonal line” is redundant.

The sentence has been removed.

10066, line 25: Please spell out “DA” as “data assimilation” since DA is not previously defined yet.

Corrected.

10067, line 3: Figure 2 -> Figure 4.

Corrected.

10067, line 4: Fig. 2a -> Fig. 4a.

Corrected.

10067, line 8: Fig. 2b -> Fig. 4b.

Corrected.

10067, line 8, “all standard deviations significantly decrease”: The decrease of NO<sub>3</sub> is not significant.

The sentence has been change to: “all standard deviations decrease in different degrees” (Line 367).

10069, line 8: There are many other flights available. Why was this flight chosen over all the others? More description on the flight observations is needed as well.

We have added all flight events that performed during May 15 to 00UTC of June 14, 2010. We chose the case of June 3 for the aircraft observations are enough and the aircraft tracks around Los Angeles, the center of model domain. For the other cases, there are not enough aircraft observations during the assimilation time windows ( $\pm 1.5$  hour of initial time), or the flight tracks are relative few and not around Los Angeles (Fig. 8). But, to demonstrate the robustness of our DA system, we run all cases and calculate the average improvements.

10069, line 25: WRf/Chem -> WRF-Chem. Note that the WRF/Chem is better changed to WRF-Chem in the entire paper.

All “WRF-Chem” have been change to “WRF/Chem”.

10071, line 17: Figure 11 does NOT show “scatter plots”.

Corrected, thank you.

10071, line 19: Fig.1a -> Fig. 11a

Corrected, thank you.

10072, lines 9-10: It is not true that the data assimilation has the hypothesis of the independent control variables. The independence of control variables merely helps to simplify the background error covariance matrix.

We agree. This sentence has been removed.

10077, Table 1: Please add the name of the species to the table.

Corrected, thank you (Page 33).

10079, Figure 2: Why aren't the cells identical in shape? It applies to Figure 3 too.

Figure 2 and Figure 3 have been plotted in the same shape.

10081, Figure 4, “Same as Fig. 3”: Figure 4 is quite different from Figure 3.

Corrected, thank you (line 373-374).

## **Referee #2**

This paper discusses implementation of cross-correlations between aerosol variables in a variational data assimilation (DA) system via balance constraint. The authors describe their methodology and then apply their new developments for a single 24-hr forecast over Southern California. Results suggest that incorporating cross-correlations within the DA system was beneficial, especially for 3- to 18-hr forecasts.

This paper is generally interesting and good, although there are some shortcomings that I believe should be addressed before publication. My biggest concerns regard that only one forecast was produced and lack of discussion about other methods of dealing with cross-correlations for aerosols, such as ensemble-based DA methods. Additionally, there are many areas of text that I believe require some clarification.

Thank you very much for your careful review and constructive suggestions. Please find below our detailed responses to all questions and comments.

## **Bigger comments, questions, and concerns**

1. I appreciate that you actually implemented your developments in a DA system to see the real-world impacts. However, you only showed results from one forecast, which does not give much confidence regarding the generality or strength of the results. If possible, I strongly urge you to add more cases. I know that adding more cases requires more work, but doing so would not add much to the length of the paper and would make the conclusions much more robust.

We agree that single one case is not convincing to show the capability of our DA system, though the major purpose is to develop the DA system with the cross-correlation process. We have added more cases in the revised manuscript, all nine flight cases from May 15 to June 14, 2010, are applied to DA experiments.

The details of these nine cases are in Table 2 and Figure 8. The results are showed in Figure 11 and Figure 12. The averaged improvement of DA for these nine cases is lower than that for the case on June 3, 2010. The main reasons are that the flight tracks are relative fewer in some cases, or the flight tracks are not around Los Angeles. Another reason is that the initial fields of Control experiment are consistent with observations, especially for the initial time at 00 UTC and 18 UTC. In the case that limited improvements were obtained at the initial fields, the improvements of subsequent forecasts are also low.

2. In my opinion, you neglected to discuss another (and easier) method of dealing with cross-correlations between aerosol species: ensemble-based DA methods (such

as the ensemble Kalman filter) that naturally handle cross-correlations. Thus, I strongly believe you should mention ensemble DA methods in the introduction, and you should cite and briefly discuss Pagowski and Grell (2012) and Schwartz et al. (2014), who assimilated aerosol observations, including PM<sub>2.5</sub>, with ensemble-based DA methods. There are other references that have also assimilated aerosol observations with ensemble DA, but I believe those two are the most relevant, and without this material regarding ensemble DA, I believe your work is not placed within its proper context.

Thanks. These two papers have been cited, and some discussions about ensemble DA methods are added in the revised manuscript (lines 109-111).

3. In light of the above comment, I believe your title should be more specific, and I suggest adding the word “variational” before “data assimilation”.

We agree. The title has been revised.

4. You left out a few important details about the DA system. For example, what DA system were you using? Was it GSI or some other system? Please briefly explain somewhere in the text. Additionally, for your 24-hr forecast you described in section 5, what was the background for DA? Finally, please briefly state the observation errors that you used.

Firstly, this DA system is not GSI or some other widely used systems. It was developed by Li et al. (2013) for the MOSAIC scheme of WRF/Chem model. A simple description about the DA system was added in Section 1 (line 129-130).

Secondly, the backgrounds for DA are the forecasting results from the previous runs without DA. These previous forecasting results have been obtained when we run the model for the BEC statistics. We added the description of the background in Section 5.1 (lines 471-473).

Thirdly, we assume that the observation error is the half of background errors. And a vertical profile of observation errors was applied, resulted from the average of background errors of every level. We think it is an enough large error, even the representativeness error is considered. Since the purpose of this manuscript is to demonstrate the signification of balance constrains in the 3DVAR system, the observation error has an insignificant impact on the analysis of balance constrains. We added the description of the observation error in Section 5.1 (lines 473-475).

5. I believe some aspects regarding Eqs. (6-13) need clarification.

a) Page 8, line 9: Please clarify what you mean by “first variable”.

The “first variable” means this variable is fixed. There is not unbalanced component for this variable that is similar to the variable of the vorticity in the DA system of ECMWF (Derber and Bouttier, 1999). But, we did not find the name of “first variable”

in other relevant literatures. Thus, we have removed this name in the revised manuscript.

b) Page 8, Eq. (7): Please fill-in the upper triangle of  $\mathbf{K}$ . Are all upper-triangle elements zero?

Yes, all upper-triangle elements are zero. We have filled in the matrix.

c) Page 8, line 19: Please clarify what you mean by “a one regression coefficient.”

It is a mistake. It should be “a regression coefficient”. We have revised this sentence.

d) Some more details about how you compute  $\rho_{ij}$  would be beneficial.

The  $\rho_{ij}$  is the statistical regression coefficients between the variables  $i$  and  $j$ . For example  $\rho_{12}$  is the regression coefficient between  $\delta EC$  and  $\delta OC$ . Here,  $\delta EC$  and  $\delta OC$  are estimated from the forecast differences of 24 h and 48 h forecasts of one month (May 15 to June 14, 2010), that is  $\delta EC = EC^{24} - EC^{48}$ ,  $\delta OC = OC^{24} - OC^{48}$ . Similar to the calculation of the BEC,  $\delta EC$  and  $\delta OC$  are also estimated by this forecast difference to represent the difference between real state and forecasts. Using the forecast difference, we have 30 pairs  $\delta EC$  and  $\delta OC$  for each grid. Then, we can estimate a regression equation and obtain the regression coefficient  $\rho_{21}$ . Since the  $\rho_{21}$  of each grid are close, we use the data of  $\delta EC$  and  $\delta OC$  at all grids to estimate a regression equation and obtain a regression coefficient  $\rho_{21}$ . This  $\rho_{21}$  should be more robust. Figure 1 shows the scatter plots of  $\delta EC$  and  $\delta OC$  for all grids. The size of  $\delta EC$  or  $\delta OC$  is  $(N \times 30)$ , where  $N$  is the number of model grid points, and 30 represents 30 days. From this scatter plots, we can obtain the regression equation:

$$\widehat{\delta OC} = 0.9 \times \delta EC. \quad (1)$$

$\widehat{\delta OC}$  is the predict of  $\delta OC$ , that is  $\delta OC_b$ . The residuals are  $\delta OC_u$ . In this equation, the intercept is neglected, since  $\delta OC$  and  $\delta EC$  are forecast differences that can be considered to be zero mean values. Using  $\delta NO_3$ ,  $\delta EC$  and  $\delta OC_u$ , we can estimate the regression equation to predict  $\delta NO_{3b}$ , and obtain  $\rho_{31}$  and  $\rho_{32}$ .

$$\delta NO_{3b} = \widehat{\delta NO_3} = \rho_{31} \delta EC + \rho_{32} \delta OC_u. \quad (2)$$

Then, the other regression equations and regression coefficient can be obtain step by step. Some more detail about the calculation of  $\rho_{ij}$  was added in the revised manuscript (lines 327-331).

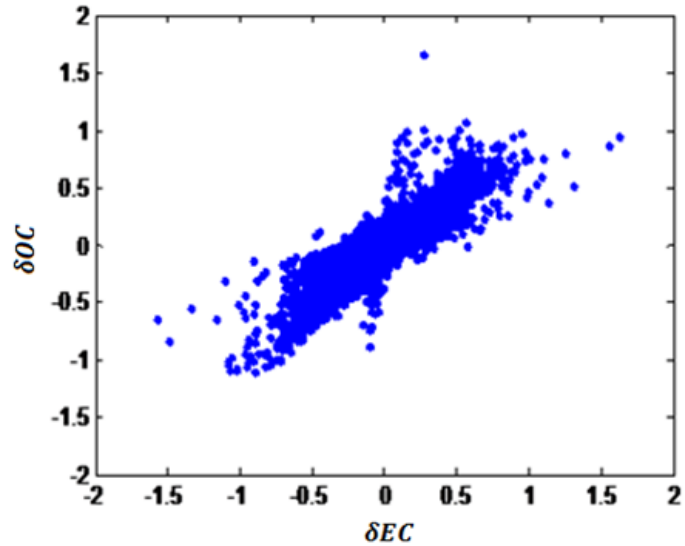


Figure 1 Scatter plots of  $\delta EC$  and  $\delta OC$

e) Additionally, I think it would be nice if you provided some details on how to interpret  $\rho_{ij}$  to bolster the discussion on page 14.

We agree. Some details of the calculation of  $\rho_{ij}$  are added in the revised manuscript (lines 327-331).

f) What would happen if the regression was not “based” on EC? In other words, what would happen if you listed the control vector species in reverse [such that OTR was in the first row on the LHS of Eq. (7) and EC was in the last row]? You mention some of this on page 14 lines 6-8, but I believe a clear description about the “order” or “first and second variables” would be greatly beneficial. You also mention using OTR as the “last variable” (page 14, line 19), but the rationale for this choice is not obvious to me. Please clarify.

We think it is difficult to clarify this question which is beyond the scope of current study. We set this order of species mainly due to the following two reasons. First, the correlation of EC and OC is the highest. Second, OTR is correlative with all other variables. The purpose of the balance constrain is to obtain as independent variables as possible. So, EC and OC should be the first two for their high correlation. If we set the other variable such as OTR as the first order, and OC as the second order, the coefficient of determination of the regression equation of OC will be less, compared with the coefficient of determination of the regression equation with EC as the first order. It will increase the correlation of  $OC_u$  with the other variables. Similarly, since OTR includes many species that are correlative with former variables, the coefficient of determination of the regression equations of OTR will be largest using all former variables as factors, and then obtain the more independent  $OTR_u$ . To investigate the impacts by using different orders, more tests need to be conducted which we may address in later studies.

In addition, we can refer other DA system to understand this question. In the formulation of DA of ECMWF (Derber and Bouttier, 1999), The balance operator  $\mathbf{K}$  matrix which transforms  $[\zeta, \eta_u, (T, P_s)_u, q]$  into  $[\zeta, \eta, (T, P_s), q]$ . The first variable is the vorticity  $\zeta$  The balanced part of the divergence  $\eta$  and the temperature and surface pressure  $(T, P_s)$  are given by the equations:

$$\eta_b = \mathbf{M}\zeta, \quad (3)$$

$$(T, P_s)_b = \mathbf{N}\zeta + P\eta_u. \quad (4)$$

Then, the  $\mathbf{K}$  matrix becomes:

$$\mathbf{K} = \begin{bmatrix} \mathbf{I} & \mathbf{0} & \mathbf{0} & \mathbf{0} \\ \mathbf{M} & \mathbf{I} & \mathbf{0} & \mathbf{0} \\ \mathbf{N} & \mathbf{P} & \mathbf{I} & \mathbf{0} \\ \mathbf{0} & \mathbf{0} & \mathbf{0} & \mathbf{I} \end{bmatrix}. \quad (5)$$

In this DA system of ECMWF, the  $\zeta$  and  $\eta$  are the first two variables. We think the reason is that they are relative high correlative. The  $(T, P_s)$  is the third variable, since it is correlative with the former variables. The  $q$  is the last variable that is not correlative with the other variables. Unfortunately, Derber and Bouttier (1999) did not explain why they set this order of variables. We explain it from our thought.

In another reference about the study of balance constraints for GSI system (Chen et al., 2013), the order of control variables is the stream function ( $\psi$ ), the unbalanced part of the velocity potential ( $\chi_u$ ), the unbalanced part of temperature ( $T_u$ ), the unbalanced part of surface pressure ( $p_{s_u}$ ), and the relative humidity ( $rh_u$ ). Here,  $rh_u$  is the last order, and its regression equation uses all former variables as factors.

g) Page 9, line 1: I feel like the word “deduced” to describe  $\rho_{21}$  is inaccurate. How exactly are you obtaining  $\rho_{ij}$ ?

The “deduced” has been changed to “obtained” (line 362). Please see the response of d) for the process of obtaining  $\rho_{ij}$ .

h) Page 9, lines 3-10: I found  $\epsilon$  confusing and also unnecessary. By definition,  $\epsilon = \delta\text{OCu}$ , so why not just use  $\delta\text{OCu}$  directly in place of  $\epsilon$ ? Thus, I suggest removing all instances of  $\epsilon$ .

We wrote Eq. (8) and reserve residual  $\epsilon$  because it is a normal format for a regression equation. This may be easier to understand for the reader. And we revised the Eq. (9) and its explanation to understand easily the calculation of  $\delta\text{OC}_b$  and  $\epsilon$  (line 215).

i) Page 9, Eq. (11). I believe you’re missing “ $\delta$ ” on EC and OCu.

Corrected, thank you.

### Smaller comments, questions, and concerns

1. Page 2, line 14: Please clarify what you mean by “coincident”.  
We mean the PM<sub>2.5</sub> concentrations of the experiment with balance constraints are more consistent with the observed concentrations. The sentence has been removed.
2. Page 2, line 17: Please omit the word “significant” because you did not perform any statistical significance testing, and you only showed results from one forecast.  
Thanks, the sentence has been revised.
3. Page 2, line 21: Again, omit “significantly”.  
Thanks, the sentence has been revised.
4. Page 2, line 26: Technically, the observation errors also determine the analysis increments.  
Thanks, the observation error has been added in the revised manuscript (line 65).
5. Page 3, line 5: Most models now have a state size  $O(10^7)$ . Suggest modifying.  
Thanks, the sentence has been revised (lines 69).
6. Page 3, lines 3-8: Note that with ensemble DA methods, these issues are not as difficult to deal with.  
Thanks, we add the qualifier of “variational data assimilation system” (line 99).
7. Page 3, line 12: Please define in words what you mean by PM<sub>2.5</sub>.  
Thanks, the definition of PM<sub>2.5</sub> has been added in the revised manuscript (lines 105).
8. Page 3, line 13: Suggest spelling out GSI and adding a reference.  
We have spelled out GSI in the revised manuscript (line 77).
9. Page 4, lines 9-11: Do these assumptions only apply to variational approaches?  
Yes. We add the qualifier of “variational” in the revised manuscript (line 99).
10. Page 4, line 20: This might be a good place to mention Pagowski and Grell (2012) and Schwartz et al. (2014).  
Thanks, we have cited these two references at lines of 109-110.
11. Page 5, line 1: Please spell out “AOD”.  
Thanks, the sentence has been revised (line 119).
12. Page 5, line 4: Please clarify what you mean by “not adjacent”.

“that are not ADJACENT” means that are not the connecting. This sentence has been revised (line 121-122).

13. Page 5, line 10: Please clarify what you mean by “eight/four”.

The MOSAIC scheme offers flexibility in specifying the number of size bins, four or eight bins are commonly used. Four bins used are located between 0.039–0.1  $\mu\text{m}$ , 0.1–1.0  $\mu\text{m}$ , 1.0–2.5  $\mu\text{m}$ , and 2.5–10  $\mu\text{m}$ . Some introductions of “eight/four” size bins have been added in the revised manuscript (lines 127-128).

14. Page 5, line 12: Suggest “developed” rather than “estimated”.

Thanks, the sentence has been revised.

15. Page 6, Eq. (1): It should be  $J(x)$  not  $J(\delta x)$ .

Thanks, the sentence has been revised (line 159).

16. Page 6, lines 20-25 and Eq. (2): You’ve ignored non-linear  $H$  and its linearization about the background to derive the linear  $H$ . In Eq. (1),  $H$  is nonlinear, but in Eq. (2) it’s linear, because you’ve linearized  $H$  about  $x_b$ . Please be more precise.

Thanks. In this paper, the observation variables are the species concentration and total PM2.5 concentration. They are really linear relationship with the state variables. Anyway, we have added the assumption of linear in the revised manuscript (line 163).

17. Page 7, line 2: In the expression for the innovation, here  $H$  should be nonlinear ( $H$ ).

Since the relationship between observation variables and state variables is linear. We do not emphasize the nonlinear  $H$ .

18. Page 7, line 7: Again, it should probably be  $10^7$  rather than  $10^6$ . Also,  $10^{12}$  should probably be  $10^{14}$ .

Thanks, the sentence has been revised (lines 174).

19. Page 7, line 14: Please clarify what you mean by “is commonly simplified with vertical levels.”

The standard deviation matrix ( $D$ ) is a diagonal matrix with the size of  $(N \times m)^2$ , that is, each species at each grid has a value of standard deviation. But, to reduce the computational cost, we use the average value of standard deviations that are at the same vertical level. Though the size of  $D$  is fixed, the number of parameters of standard deviations reduces in the DA system. We have added some introduction in the revised manuscript (lines 180-181).

20. Page 10, lines 8-9: It was unclear to me how you got Eq. (17) from Eq. (6).

Please add some steps or clarify.

According to the definition of the BEC,

$$\mathbf{B} = \langle (\delta \mathbf{x})(\delta \mathbf{x}^T) \rangle.$$

Using Eq. (6),

$$\begin{aligned} \mathbf{B} &= \langle (\mathbf{K}\delta \mathbf{x}_u)(\mathbf{K}\delta \mathbf{x}_u)^T \rangle \\ &= \langle (\mathbf{K}\delta \mathbf{x}_u)(\delta \mathbf{x}_u^T \mathbf{K}^T) \rangle \\ &= \mathbf{K}\mathbf{B}_u\mathbf{K}^T \end{aligned}$$

Some explains have been added in the revised manuscript (lines 237-242).

21. Page 11, line 1: In Eq. (20), it appears you used  $\delta \mathbf{x} = \mathbf{B}^{1/2}\delta \mathbf{z}$ . Thus, I believe line 1 on page 11 should read  $\delta \mathbf{z} = \mathbf{B}^{-1/2}\delta \mathbf{x}$  (note the negative sign on the exponent of B). Please double-check.

Corrected, thank you.

22. Page 12, line 5: Should be “horizontal grid spacing” not “resolution”...they mean different things.

Thanks, the sentence has been revised (lines 274).

23. Page 12, lines 10-12: Please clarify what you mean by “former forecast”. Additionally, where do the initial meteorological conditions come from? Are these also from NARR?

The initial meteorological condition is from NARR. For a 48-hour or 24-hour forecast running, we update the initial meteorological condition using the reanalysis NARR data. But for the initial aerosol condition, since there are not reanalysis data, we use the forecast condition from former forecast as the initial condition. The explanation has been added in the revised manuscript (line 281-283).

24. Page 12, line 26 and page 13, line 2: I wonder if you might want to rename “E\_ORG” to “E\_OC” and “E\_PM25” to “E\_OTR” to be consistent with the nomenclature of the control variables. If so, please also change on the relevant figure (Fig. 2) and elsewhere in the text.

Since the emission variables are different with the model control variables. The former include many aerosol precursors such as E\_SO2, E\_NO2. These aerosol precursors can transform into aerosol through chemical process. Thus, the emission variable E\_SO4 or E\_NO3 are not completely corresponding to the control variables. We use the name of emission variables, consistent with the name in user’s guide of WRF/Chem.

25. Page 13, line 5: “With the exception” is misleading and suggests that the diagonal correlations will be  $< 0.5$ . Please modify.

We have modified the corresponding sentence in the revised manuscript (Line 305).

26. Page 13, line 9: Suggest “high” rather than “close”.

Corrected.

27. Page 14, line 1: I believe it should be Eqs. (6-13) rather than Eqs. (6-12).

Corrected.

28. Page 14, line 2: I believe Eq. (7) is more correct than Eq. (6).

Corrected.

29. Page 14, lines 9-19: Should the control variables here have subscripts “u”? I’m not sure. Please double-check.

We have double-checked.

30. Page 14: Just a comment—I really like Fig. 3.

Thanks.

31. Page 15, line 2: Suggest “obtained” rather than “performed”.

Corrected.

32. Page 15, lines 2, 3, and 8: In all these locations, it should be Fig. 4, not Fig. 2.

Corrected, thanks.

33. Page 15, lines 10-11: I believe OTR and NO<sub>3</sub> should be OTR<sub>u</sub> and NO<sub>3u</sub>, respectively.

Corrected.

34. Page 15, lines 10-11: Please clarify with what the “decreases” are with respect to.

Thanks, we have modified the sentence (Line 369)

35. Page 15, line 17: I believe it should be Eq. (22), not Eq. (21).

Corrected.

36. Page 15, lines 18-25: Please explain how you get the horizontal correlation scale (L<sub>s</sub>) from Fig. 5. Is L<sub>s</sub> defined as an e-folding distance? Overall, I was a bit confused by your description of L<sub>s</sub>—please clarify.

We assume that the decline curve of horizontal correlations is according to the Gaussian function (Fig. 5). Then the intersection of the decline curve and the line of  $e^{-\frac{1}{2}}$  ( $\approx 0.61$ ) can be approximately as the value of horizontal correlation scale. The introduction has been added in the revised manuscript (lines 384-386).

37. Page 15, line 27: I believe OC, NO<sub>3</sub>, SO<sub>4</sub>, and OTR should have subscript “u”.

Corrected.

38. Page 16, line 1: Please clarify what you mean by “common factors in regression equations”.

The common factors mean EC, OC<sub>u</sub>, and NO<sub>3u</sub>. For example, EC is used four times in the regression Eqs. (6-13), OC<sub>u</sub> is used three times, NO<sub>3u</sub> is used two times. But, it may be puzzling to readers. We have revised this sentence in the manuscript (lines 390-391).

39. Page 16, lines 4-16: Similar to my above comment, please explain how you get the vertical correlation length-scales from Fig. 6.

For the vertical correlation, we use the real values calculated from the forecasting differences in the DA system, but not approximate values from an alternative function. The name of “vertical correlation length-scale” is just a conception to explain the difference between the unbalanced variables and full variables. We have added some explanations in the revised manuscript (lines 397-399, 405-406)

40. Page 16, lines 13-16: I only see very small differences regarding the vertical correlations between the full and unbalanced variables. Perhaps you may wish to modify the text.

The differences of vertical correlation are slight, compared with the difference of horizontal. The main reason is that the vertical correlations are generally affected by the atmospheric boundary layer height. Thus, all vertical correlation decreases rapidly for the level above the boundary layer height. We have added this explanation in the revised manuscript (lines 410-413).

41. Page 17, line 23: Please clarify that DA-balance assimilates the same observations as “DA-full”.

For the DA-full experiments and DA-balance experiments, we use the same observation for the data assimilation. This sentence has been revised (lines 469-470).

42. Page 17, line 25: “WRF” not “WRf”.

Thanks, the sentence has been revised.

43. Page 17, line 28: Please clarify what you mean by “the initial time”.

The initial time means the start time of the model running, which is listed in Table 2.

44. Page 18, lines 4-26: I feel like this discussion slightly misses the main points. In

my opinion, the main point is that the balance constraints can allow observations of a specific species to impact other variables. Even with PM2.5 observations, because the model-simulated PM2.5 is a function of all the control variables, the individual species' fields are adjusted through the BECs, even without a direct observation of the individual species. Thus, without multivariate correlations, an aircraft observation of OC can only impact OC (because the forward operator for OC is only a function of OC), but with the multivariate BECs, an OC observation can now impact OTR or EC. Perhaps you might wish to clarify some aspects of the text along these lines.

Yes. For the BECs without balance constraints, the observation of OC can only impact OC. The crossing effects among species from the BECs with balance constraints. This section has been revised (lines 484-489).

45. Page 19, lines 1-5: I don't believe it is appropriate to describe the smaller RMSEs as "improvements". You're simply looking at fits to observations, which, on their own, do not tell you anything about the relative goodness of your DA system.

The comparison between the analysis PM2.5 against the assimilated observations is known as "sanity check". It can demonstrate the capability of the DA system. In the revised manuscript, we use more data from all nine cases to demonstrate the effects of the DA system. This section has been revised (lines 506-517).

46. Page 19, line 17: The description here of Fig. 11 is incorrect.

Corrected.

47. Page 19, line 19: It should be Fig. 11a, not 1a.

Corrected.

48. Page 19, line 20: Omit "significantly". You can maybe replace it with "substantially".

Thanks, the sentence has been revised.

49. Page 20, lines 16-17: Please clarify what you mean by these lines.

This sentence means the horizontal correlation scales of unbalanced variables are closer than that of full variables. And the vertical correlation scales show similar trend. The sentence has been revised (lines 556-558).

50. Page 20, line 27: Please clarify what you mean by "mutual spread".

The "mutual spread" has been changed to "crossing spread" (line 489).

51. Page 21, line 6: I don't agree with this line. You're only looking at the analysis fits, which does not mean your analysis fields are necessarily better.

This sentence has been removed in the revised manuscript.

52. Page 21, line 20: Please clarify what you mean by a “universal balance constraint”.

The balance constraint in this paper is just a statistical relationship. We hope to find a universal balance that can describe the physical or chemical balanced relationship of aerosol variables, similar with the balance constraint of geostrophic balance or temperature-salinity balance in meteorological or oceanic data assimilation. The sentence has been revised in the manuscript (lines 585-586).

53. Table 1: Suggest also pointing to Eq. (7) in the caption. Also, you should annotate the various species on this figure somehow, because it’s difficult to look back to Eq. (7).

Thanks, we followed this suggestion.

54. Fig. 2 caption: Suggest “NEI05” rather than just “NEI”

Thanks, the sentence has been revised.

55. Fig. 4 caption: In my opinion, this figure isn’t that close to Fig. 3 so I suggest elaborating.

Corrected, thank you .

56. Fig. 5 caption: Suggest pointing to Fig. 4 rather than Fig. 3.

Corrected.

57. Fig. 6: Suggest adding labels of “Height” to the axes.

Corrected.

58. Fig. 7: Suggest adding a unit (meters) to the colorbar.

Corrected.

59. Figs. 8 and 9: The labels above/below the panels are very small. Can these be enlarged?

Corrected.

1 **Background error covariance with balance constraints for aerosol species and**  
2 **applications in **variational** data assimilation**

3  
4  
5  
6  
7  
8  
9  
10  
11  
12  
13  
14  
15  
16  
17  
18  
19  
20  
21  
22  
23  
24  
25  
26  
27  
28  
29  
30  
31  
32  
33

Zengliang Zang<sup>1</sup>, Zilong Hao<sup>1</sup>, Yi Li<sup>1</sup>, Xiaobin Pan<sup>1</sup>, Wei You<sup>1</sup>, Zhijin Li<sup>2</sup> and Dan Chen<sup>3</sup>

Units: <sup>1</sup> College of Meteorology and Oceanography, PLA University of Science and Technology,  
Nanjing 211101, China;

<sup>2</sup>Joint Institute For Regional Earth System Science and Engineering, University of California, Los  
Angeles, California90095, USA;

<sup>3</sup>National Center for Atmospheric Research, Boulder, Colorado 80305, USA

Jun 8, 2016

Corresponding author:  
Prof. Zengliang Zang  
E-mail: zzlqxy@163.com  
Telephone: 86-025-80830400  
Fax: 86-025-80830400  
Address: No.60, Shuanglong Street, Nanjing 211101, China

34 **Abstract**

35 Balance constraints are important for background error covariance (BEC) in data assimilation  
36 to spread information between different variables and produce balance analysis fields. Using  
37 statistical regression, we develop a balance constraint for the BEC of aerosol variables and apply it  
38 to a three-dimensional variational data assimilation system in the WRF/Chem model. One-month  
39 forecasts from the WRF/Chem model are employed for BEC statistics. The cross-correlations  
40 between the different species are generally high. The largest correlation occurs between elemental  
41 carbon and organic carbon with as large as 0.9. After using the balance constraints, the  
42 correlations between the unbalanced variables reduce to less than 0.2. A set of data assimilation  
43 and forecasting experiments is performed. In these experiments, surface PM<sub>2.5</sub> concentrations and  
44 speciated concentrations along aircraft flight tracks are assimilated. The analysis increments with  
45 the balance constraints show spatial distributions more complex than those without the balance  
46 constraints, which is a consequence of the spreading of observation information across variables  
47 due to the balance constraints. The forecast skills with the balance constraints show substantial  
48 and durable improvements from the 2<sup>nd</sup> hour to the 16<sup>th</sup> hour compared with the forecast skills  
49 without the balance constraints. The results suggest that the developed balance constraints are  
50 important for the aerosol assimilation and forecasting.

51 **Keyword:** aerosol species, WRF/Chem, data assimilation, balance constraint, background error  
52 covariance

53

54

55

56

57

58

59

60

61 **1. Introduction**

62 Aerosol data assimilation in **chemical transport models** has received an increasing amount of  
63 attention in recent years as a basic methodology for improving aerosol analysis and forecasting. In  
64 a data assimilation system, the background error covariance (BEC) plays a crucial role in the  
65 success of an assimilation process. **The BEC and the observation error** determine analysis  
66 increments from the assimilation process (Derber and Bouttier 1999, Chen et al., 2013).

67 However, accurate estimation of the BEC remains difficult due to a lack of information about  
68 the true atmospheric states and also due to computational requirement arising from the large  
69 dimension of the BEC (typically  $10^7 \times 10^7$ ). **For a variational data assimilation system,** a few  
70 methods have been developed to estimate and simplify the expression of the BEC, such as the  
71 analysis of innovations, the NMC (National Meteorological Center) and the ensemble-based  
72 (Monte Carlo) methods. The NMC method is extensively used in operational atmospheric and  
73 meteorology-chemistry data assimilation systems. It assumes that the forecast errors are  
74 approximated by differences between pairs of forecasts that are valid at the same time (Parrish and  
75 Derber, 1992). Pagowski et al. (2010) estimated the BEC of PM<sub>2.5</sub> **(particles having an**  
76 **aerodynamic diameter less than 2.5 μm)** by calculating the differences between the forecasts of 24  
77 and 48 h, and used the estimated BEC in a **Grid-point Statistical Interpolation (GSI) system (Wu et**  
78 **al., 2002)**. Benedetti et al. (2007) estimated the BEC of the sum of the mixing ratios of all aerosol  
79 species for an operational analysis and forecast systems at ECMWF (The European Centre for  
80 Medium-Range Weather Forecasts). The BEC with multiple species and size bins of aerosols have  
81 been calculated and employed in data assimilation. Liu et al. (2011) estimated the BEC with 14  
82 aerosol species in the Goddard Chemistry Aerosol Radiation and Transport scheme of the Weather  
83 Research and Forecasting/Chemistry (WRF/Chem) model and applied it to the GSI system.  
84 Schwartz et al. (2012) increased the number of the species to 15 based on the study of Liu et al.  
85 (2011). Li et al. (2013) estimated the BEC for five species derived from the Model for Simulation  
86 Aerosol Interactions and Chemistry (MOSAIC) scheme.

87 One important role that the BEC plays in meteorological data assimilation is to spread  
88 information between different variables to produce **balanced** analysis fields, which employ  
89 balance constraints to convert original variables into new independent variables. Balance

90 constraints have been employed in atmospheric and oceanic data assimilation, such as geostrophic  
91 balance or temperature-salinity balance (Bannister, 2008a, 2008b). To incorporate balance  
92 constraints, the model variables are usually transformed to balanced and unbalanced parts. The  
93 unbalanced parts as control variables are can be assumed independent, and the balanced parts are  
94 constrained by balance constraints (Derber and Bouttier, 1999). Instead of using an empirical  
95 function as a balance constraint, balance constraints are also derived using regression techniques  
96 (Ricci and Weaver, 2005). Although distinct empirical relations between some variables (such as  
97 temperature and humidity) may not exist, the regression equation can also be estimated as balance  
98 constraints (Chen et al., 2013).

99 In current aerosol **variational** data assimilation with multiple variables, balance constraints are  
100 not yet incorporated in the BEC. The state variables are assumed to be independent variables  
101 without cross-correlation. However, the aerosol species are frequently highly correlated due to  
102 their common emission sources and diffusion processes. For example, the correlations in terms of  
103 the R-square between elemental carbon and black carbon exceed 0.6 in many locations across Asia  
104 and the South Pacific in both urban and suburban locations (Salako et al., 2012), and the  
105 correlations between different size bins, such as **PM<sub>2.5</sub> and PM<sub>10-2.5</sub> (the diameter of particles being**  
106 **between 2.5 and 10 μm)**, are also generally significant (Sun et al., 2003; Geller et al., 2004). Thus,  
107 the cross-correlations between different **species or size bins** are necessary to produce balanced  
108 analysis fields. Cross-correlations spread the observation information from one variable to other  
109 variables, which **can produce more balanced initial fields.** **For the data assimilation of the**  
110 **ensemble Kalman filter method, the BEC with balance constraints is assured (Pagowski et al.,**  
111 **2012; Schwartz et al., 2014), although the balance may break down because of localization.**

112 Recently, several studies have suggested that the BEC with balanced cross-correlation should  
113 be introduced into aerosol variational data assimilation (Kahnert, 2008; Liu et al., 2011; Li et al.,  
114 2013; Saide et al., 2013). Kahnert (2008) exhibited cross-correlations of the seventeen aerosol  
115 variables from Multiple-scale Atmospheric Transport and Chemistry (MATCH) Model. He found  
116 that the statistical cross-correlations between aerosol components are primarily influenced by the  
117 interrelations between emissions and by interrelations due to chemical reactions to a much lesser  
118 degree. Saide et al., (2012; 2013) incorporated the capacity to add cross-correlations between

119 aerosol size bins in GSI for assimilating observations of aerosol optical depth (AOD) data. The  
120 cross-correlations between the two connecting size bins for each species were considered using  
121 recursive filters while, the cross-correlation is not considered for the other size bins that are not  
122 connecting.

123 In this paper, we explore incorporating cross-correlations between different species in BEC  
124 using balance constraints. The balance constraints are established using statistical regression. We  
125 apply the BEC with the balance constraints to a data assimilation and forecasting system with the  
126 MOSAIC scheme in WRF/Chem. The MOSAIC scheme includes a large number of variables with  
127 eight species, and flexibility of eight or four size bins. The scheme of four size bins is used in our  
128 studies. The four bins are located between 0.039–0.1  $\mu\text{m}$ , 0.1–1.0  $\mu\text{m}$ , 1.0–2.5  $\mu\text{m}$ , and 2.5–10  $\mu\text{m}$ ,  
129 and the total mass of the first three bins are PM<sub>2.5</sub>. A 3DVAR system for the MOSAIC (4-bin)  
130 scheme has been developed by Li et al. (2013). For comparisons, we employ this 3DVAR system  
131 with the same model configurations as employed by Li et al. (2013). The data assimilation and  
132 forecasting experiments are performed with a focus on assessing the impact of cross-correlations  
133 of the BEC on analyses and forecasts.

134 The paper is organized as follows: Section 2 describes the 3DVAR system and the formulation  
135 of the BEC. Section 3 describes the WRF/Chem configuration and estimates the correlations  
136 among the emissions. The statistical characteristics of the BEC, including the regression  
137 coefficient of the cross-correlation, are discussed in Section 4. Using the BEC, experiments of  
138 assimilating surface PM<sub>2.5</sub> observations and aircraft observations are discussed in Section 5.  
139 Shortcomings, conclusions and future perspectives are presented in Section 6.

## 140 2. Data assimilation system and BEC

141 In this section, we present a formulation of the BEC with cross-correlation between different  
142 species using a regression technique. Then, the cost function with the new BEC is derived and the  
143 calculating factorization of the BEC is described.

144 The control variables of the data assimilation are obtained from the MOSAIC (4-bin) aerosol  
145 scheme in the WRF/Chem model (Zaveri et al., 2008). The MOSAIC scheme includes eight  
146 aerosol species, that is, elemental carbon or black carbon (EC/BC), organic carbon (OC), nitrate  
147 (NO<sub>3</sub>), sulfate (SO<sub>4</sub>), chloride (Cl), sodium (Na), ammonium (NH<sub>4</sub>), and other inorganic mass

148 (OIN). Each species is separated into four bins with different sizes: 0.039–0.1  $\mu\text{m}$ , 0.1–1.0  $\mu\text{m}$ ,  
 149 1.0–2.5  $\mu\text{m}$  and 2.5–10  $\mu\text{m}$ . The scheme involves 32 aerosol variables with eight species and four  
 150 size bins. These variables cannot be directly introduced as control variables in an assimilation  
 151 system in consideration of computational efficiency. The number of variables must be decreased  
 152 prior to assimilation. Li et al. (2013) have lumped these variables into five species as control  
 153 variables in the 3DVAR system. The five species consist of EC, OC,  $\text{NO}_3$ ,  $\text{SO}_4$  and OTR. Here,  
 154 OTR is the sum of Cl, Na,  $\text{NH}_4$  and OIN. Note that the data assimilation system aims to assimilate  
 155 the observation of  $\text{PM}_{2.5}$ ; only the first three of four size bins are utilized to lump as one control  
 156 variable for each species.

157 For a 3DVAR system, the cost function ( $J$ ), which measures the distance of the state vector to the  
 158 background and observations, can be written as follows:

$$159 \quad J(\mathbf{x}) = \frac{1}{2}(\mathbf{x} - \mathbf{x}^b)^T \mathbf{B}^{-1}(\mathbf{x} - \mathbf{x}^b) + \frac{1}{2}(\mathbf{y} - \mathbf{H}\mathbf{x})^T \mathbf{R}^{-1}(\mathbf{y} - \mathbf{H}\mathbf{x}). \quad (1)$$

160 Here,  $\mathbf{x}$  is the vector of the state variables, including EC, OC,  $\text{NO}_3$ ,  $\text{SO}_4$  and OTR;  $\mathbf{x}^b$  is the  
 161 background vector of these five species, which are generated by the MOSAIC scheme;  $\mathbf{y}$  is the  
 162 observation vector;  $\mathbf{H}$  is the observation operator that maps the model space to the observation  
 163 space and is assumed to be linear here;  $\mathbf{R}$  is the observation error covariance associated with  $\mathbf{y}$ ;  
 164 and  $\mathbf{B}$  is the background error covariance associated with  $\mathbf{x}^b$ . Eq. (1) is usually written in the  
 165 incremental form

$$166 \quad J(\delta\mathbf{x}) = \frac{1}{2}\delta\mathbf{x}^T \mathbf{B}^{-1}\delta\mathbf{x} + \frac{1}{2}(\mathbf{H}\delta\mathbf{x} - \mathbf{d})^T \mathbf{R}^{-1}(\mathbf{H}\delta\mathbf{x} - \mathbf{d}), \quad (2)$$

167 where  $\delta\mathbf{x}$  ( $\delta\mathbf{x} = \mathbf{x} - \mathbf{x}^b$ ) is the incremental state variable. The observation innovation vector is  
 168 known as  $\mathbf{d} = \mathbf{y} - \mathbf{H}\mathbf{x}^b$ . The minimization solution is the analysis increment  $\delta\mathbf{x}$ , and the final  
 169 analysis is  $\mathbf{x}^a = \mathbf{x}^b + \delta\mathbf{x}$ . This analysis is statistically optimal as a minimum error variance  
 170 estimate (e.g., Jazwinski, 1970; Cohn, 1997).

171 In Eq. (1) or Eq. (2),  $\mathbf{x}^b$  is a  $(N \times m)$  – vector, where  $N$  is the number of model grid points,  
 172 and  $m$  is the number of state variables.  $\mathbf{B}$  is a symmetric matrix with a dimension of  $(N \times m)^2$ .  
 173 For a high-resolution model, the number of vector  $\mathbf{x}^b$  is on the order of  $10^7$ . Therefore, the  
 174 number of elements in  $\mathbf{B}$  is approximately  $10^{14}$ . With this dimension,  $\mathbf{B}$  cannot be explicitly  
 175 manipulated. To pursue simplifications of  $\mathbf{B}$ , we employ the following factorization

176 
$$\mathbf{B} = \mathbf{D}\mathbf{C}\mathbf{D}^T, \quad (3)$$

177 where  $\mathbf{D}$  and  $\mathbf{C}$  are the standard deviation matrix and the correlation matrix, respectively.  $\mathbf{D}$   
 178 and  $\mathbf{C}$  can be described and separately prescribed after the factorization.  $\mathbf{D}$  is a diagonal matrix  
 179 whose elements include the standard deviation of all state variables in the three-dimensional grids.  
 180 To reduce the computational cost, we use the average value of standard deviations that are at the  
 181 same level. Thus, the standard deviation is simplified with vertical levels.  $\mathbf{C}$  is a symmetric  
 182 matrix, having the form

183 
$$\mathbf{C} = \begin{bmatrix} \mathbf{C}_{EC}^{EC} & \mathbf{C}_{EC}^{OC} & \mathbf{C}_{EC}^{NO_3} & \mathbf{C}_{EC}^{SO_4} & \mathbf{C}_{EC}^{OTR} \\ \mathbf{C}_{OC}^{EC} & \mathbf{C}_{OC}^{OC} & \mathbf{C}_{OC}^{NO_3} & \mathbf{C}_{OC}^{SO_4} & \mathbf{C}_{OC}^{OTR} \\ \mathbf{C}_{NO_3}^{EC} & \mathbf{C}_{NO_3}^{OC} & \mathbf{C}_{NO_3}^{NO_3} & \mathbf{C}_{NO_3}^{SO_4} & \mathbf{C}_{NO_3}^{OTR} \\ \mathbf{C}_{SO_4}^{EC} & \mathbf{C}_{SO_4}^{OC} & \mathbf{C}_{SO_4}^{NO_3} & \mathbf{C}_{SO_4}^{SO_4} & \mathbf{C}_{SO_4}^{OTR} \\ \mathbf{C}_{OTR}^{EC} & \mathbf{C}_{OTR}^{OC} & \mathbf{C}_{OTR}^{NO_3} & \mathbf{C}_{OTR}^{SO_4} & \mathbf{C}_{OTR}^{OTR} \end{bmatrix}, \quad (4)$$

184 where  $\mathbf{C}_{EC}$ ,  $\mathbf{C}_{OC}$ ,  $\mathbf{C}_{NO_3}$ ,  $\mathbf{C}_{SO_4}$  and  $\mathbf{C}_{OTR}$  at diagonal locations are the background error  
 185 auto-correlation matrices that are associated with each species. They represent the correlation  
 186 among pairs of grid points for one species. Other submatrices represent the correlations between  
 187 different species, known as cross-correlations. For example,  $\mathbf{C}_{OC}^{EC}$  represents the cross-correlations  
 188 between EC and OC, and  $\mathbf{C}_{OC}^{EC} = (\mathbf{C}_{EC}^{OC})^T$ . In Li et al. (2013), these cross-correlations were  
 189 disregarded, that is, the five species are considered independently and  $\mathbf{C}$  is thus a block diagonal  
 190 matrix.

191 In this study, the cross-correlations between different species are considered by introducing  
 192 control variable transforms (Derber and Bouttier, 1999; Barker, 2004; Huang, 2009). We divide  
 193 the model aerosol variables into balanced components ( $\delta\mathbf{x}_b$ ) and unbalanced components ( $\delta\mathbf{x}_u$ ):

194 
$$\delta\mathbf{x} = \delta\mathbf{x}_b + \delta\mathbf{x}_u. \quad (5)$$

195 Note the EC does not need to be divided. There is not unbalanced component for EC that is  
 196 similar to the variable of vorticity in the data assimilation of ECMWF (Derber and Bouttier, 1999),  
 197 or the variable of stream function in the data assimilation of MM5 (Barker, 2004). The  
 198 transformation from unbalanced variables ( $\delta\mathbf{x}_u$ ) to full variables ( $\delta\mathbf{x}$ ) by the balance operator  $\mathbf{K}$   
 199 is given by

200 
$$\delta\mathbf{x} = \mathbf{K}\delta\mathbf{x}_u. \quad (6)$$

201 Eq. (6) can be written as

$$202 \begin{bmatrix} \delta EC \\ \delta OC \\ \delta NO_3 \\ \delta SO_4 \\ \delta OTR \end{bmatrix} = \begin{bmatrix} \mathbf{I} & \mathbf{0} & \mathbf{0} & \mathbf{0} & \mathbf{0} \\ \rho_{21} & \mathbf{I} & \mathbf{0} & \mathbf{0} & \mathbf{0} \\ \rho_{31} & \rho_{32} & \mathbf{I} & \mathbf{0} & \mathbf{0} \\ \rho_{41} & \rho_{42} & \rho_{43} & \mathbf{I} & \mathbf{0} \\ \rho_{51} & \rho_{52} & \rho_{53} & \rho_{54} & \mathbf{I} \end{bmatrix} \begin{bmatrix} \delta EC \\ \delta OC_u \\ \delta NO_{3u} \\ \delta SO_{4u} \\ \delta OTR_u \end{bmatrix}, \quad (7)$$

203 where  $\rho_{ij}$  is the submatrix of  $\mathbf{K}$ , which represents the statistical regression coefficients between  
 204 the variables  $i$  and  $j$  (Chen et al., 2013). Note that  $\rho_{ij}$  is a diagonal matrix with the dimension of  
 205 model grid points. Each model grid point has a regression coefficient. For convenience, we  
 206 assumed that the elements of  $\rho_{ij}$  is a constant value for all grid points, which are denoted as  $\rho_{ij}$   
 207 and are calculated by linear regression with all grid points. For example,  $\rho_{21}$  can be obtained  
 208 from the regression equation of OC and EC as

$$209 \delta OC = \rho_{21} \delta EC + \varepsilon, \quad (8)$$

210 where  $\varepsilon$  is the residual.  $\delta EC$  and  $\delta OC$  can be estimated from the forecast differences of 24 h  
 211 forecasts and 48 h forecasts, similar to the statistics of the BEC. Eq. (8) contains the slope but no  
 212 intercept. The intercept is nearly zero because  $\delta EC$  and  $\delta OC$  represent forecast differences that  
 213 can be considered to be zero mean values. After obtaining  $\rho_{21}$ , the balanced part (e.g., the value  
 214 of the regression prediction) of  $\delta OC$  can be obtained by

$$215 \delta OC_b = \widehat{\delta OC} = \rho_{21} \delta EC. \quad (9)$$

216 Where  $\widehat{\delta OC}$  represents the predicted value of Eq. (8), which is equal to the balanced part ( $\delta OC_b$ ).  
 217 Remove the  $\delta OC_b$  from the full variables to obtain the unbalanced part ( $\delta OC_u$ ), that is,  $\varepsilon$  in Eq.  
 218 (8). Thus, the calculation of  $\delta OC_u$  can be written as

$$219 \delta OC_u = \delta OC - \rho_{21} \delta EC. \quad (10)$$

220 Here,  $\delta OC_u$  and  $\delta EC$  are employed as predictors in the next regression equation to obtain  
 221  $\delta NO_{3b}$ . Then, we can obtain the unbalanced parts of the remaining variables, which are defined as  
 222 follows:

$$223 \delta NO_{3u} = \delta NO_3 - (\rho_{31} \delta EC + \rho_{32} \delta OC_u), \quad (11)$$

$$224 \delta SO_{4u} = \delta SO_4 - (\rho_{41} \delta EC + \rho_{42} \delta OC_u + \rho_{43} \delta NO_{3u}), \quad (12)$$

$$225 \delta OTR_u = \delta OTR - (\rho_{51} \delta EC + \rho_{52} \delta OC_u + \rho_{53} \delta NO_{3u} + \rho_{54} \delta SO_{4u}), \quad (13)$$

226 The coefficient of determination ( $R^2$ ) can be employed to measure the fit of these regressions. It  
 227 can be expressed as

$$228 \quad R^2 = \frac{SSR}{SST}, \quad (14)$$

229 where SSR and SST are the regression sum of squares and the sum of squares for total,  
 230 respectively.

231 These unbalanced parts can be considered to be independent because they are residual and  
 232 random.  $\mathbf{B}_u$  denotes the unbalanced variables of the BEC and can be factorized as

$$233 \quad \mathbf{B}_u = \mathbf{D}_u \mathbf{C}_u \mathbf{D}_u^T, \quad (15)$$

234 where  $\mathbf{D}_u$  and  $\mathbf{C}_u$  are the standard deviation matrix and the correlation matrix, respectively.  $\mathbf{C}_u$   
 235 should be a block diagonal without cross-correlations as follows:

$$236 \quad \mathbf{C}_u = \begin{bmatrix} \mathbf{C}_{EC} & & & & \\ & \mathbf{C}_{OCu} & & & \\ & & \mathbf{C}_{NO_{3u}} & & \\ & & & \mathbf{C}_{SO_{4u}} & \\ & & & & \mathbf{C}_{OTRu} \end{bmatrix}. \quad (16)$$

237 According to the definition of the BEC,

$$238 \quad \mathbf{B} = \langle (\delta \mathbf{x})(\delta \mathbf{x}^T) \rangle. \quad (17)$$

239 And  $\mathbf{B}_u$  can be written as

$$240 \quad \mathbf{B}_u = \langle (\delta \mathbf{x}_u)(\delta \mathbf{x}_u^T) \rangle. \quad (18)$$

241 Using Eq. (6), Eq. (17) and Eq. (18), the relationship between  $\mathbf{B}$  and  $\mathbf{B}_u$  is

$$242 \quad \mathbf{B} = \mathbf{K} \mathbf{B}_u \mathbf{K}^T. \quad (19)$$

243  $\mathbf{B}^{\frac{1}{2}}$  and  $\mathbf{B}_u^{\frac{1}{2}}$  are defined as the square root of  $\mathbf{B}$  and the square root of  $\mathbf{B}_u$ , respectively. Their  
 244 transformation is

$$245 \quad \mathbf{B}^{\frac{1}{2}} = \mathbf{K} \mathbf{B}_u^{\frac{1}{2}}. \quad (20)$$

246 Using Eq. (15), Eq. (20) can be written as follows:

$$247 \quad \mathbf{B}^{\frac{1}{2}} = \mathbf{K} \mathbf{D}_u \mathbf{C}_u^{\frac{1}{2}}. \quad (21)$$

248 Generally, a transformed cost function of Eq. (2) is expressed as a function of a preconditioned  
 249 state variable:

250 
$$J(\delta\mathbf{z}) = \frac{1}{2}\delta\mathbf{z}^T\delta\mathbf{z} + \frac{1}{2}\left(\mathbf{H}\mathbf{B}^{\frac{1}{2}}\delta\mathbf{z} - \mathbf{d}\right)^T \mathbf{R}^{-1}\left(\mathbf{H}\mathbf{B}^{\frac{1}{2}}\delta\mathbf{z} - \mathbf{d}\right). \quad (22)$$

251 Here,  $\delta\mathbf{z} = \mathbf{B}^{\frac{1}{2}}\delta\mathbf{x}$ . Using Eq. (21), Eq. (22) can be written as

252 
$$J(\delta\mathbf{z}) = \frac{1}{2}\delta\mathbf{z}^T\delta\mathbf{z} + \frac{1}{2}\left(\mathbf{H}\mathbf{K}\mathbf{D}_u\mathbf{C}_u^{\frac{1}{2}}\delta\mathbf{z} - \mathbf{d}\right)^T \mathbf{R}^{-1}\left(\mathbf{H}\mathbf{K}\mathbf{D}_u\mathbf{C}_u^{\frac{1}{2}}\delta\mathbf{z} - \mathbf{d}\right). \quad (23)$$

253 Eq. (23) is the last form of the cost function with the cross-correlation of  $\mathbf{B}$ .

254 According to Li et al. (2013), the correlation matrix of the unbalanced parts ( $\mathbf{C}_u$ ) is factorized as

255 
$$\mathbf{C}_u = \mathbf{C}_{ux} \otimes \mathbf{C}_{uy} \otimes \mathbf{C}_{uz}. \quad (24)$$

256 Here,  $\otimes$  denotes the Kronecker product, and  $\mathbf{C}_{ux}$ ,  $\mathbf{C}_{uy}$  and  $\mathbf{C}_{uz}$  represent the correlation  
 257 matrices between gridpoints in the  $x$  direction, the  $y$  direction, and the  $z$  direction, respectively,  
 258 with the sizes  $n_x \times n_x$ ,  $n_y \times n_y$ , and  $n_z \times n_z$ , respectively. Here,  $n_x$ ,  $n_y$  and  $n_z$  represent the  
 259 numbers of grid points in the  $x$  direction,  $y$  direction, and  $z$  direction, respectively. This  
 260 factorization can decrease the size of the dimension of  $\mathbf{C}_u$ . Another desirable property of Eq. (24)  
 261 is

262 
$$\mathbf{C}_u^{\frac{1}{2}} = \mathbf{C}_{ux}^{\frac{1}{2}} \otimes \mathbf{C}_{uy}^{\frac{1}{2}} \otimes \mathbf{C}_{uz}^{\frac{1}{2}} \quad (25)$$

263  $\mathbf{C}_{ux}$  and  $\mathbf{C}_{uy}$  are expressed by Gaussian functions, and  $\mathbf{C}_{uz}$  is directly computed from the proxy  
 264 data. They will be discussed in Sec 4.2.

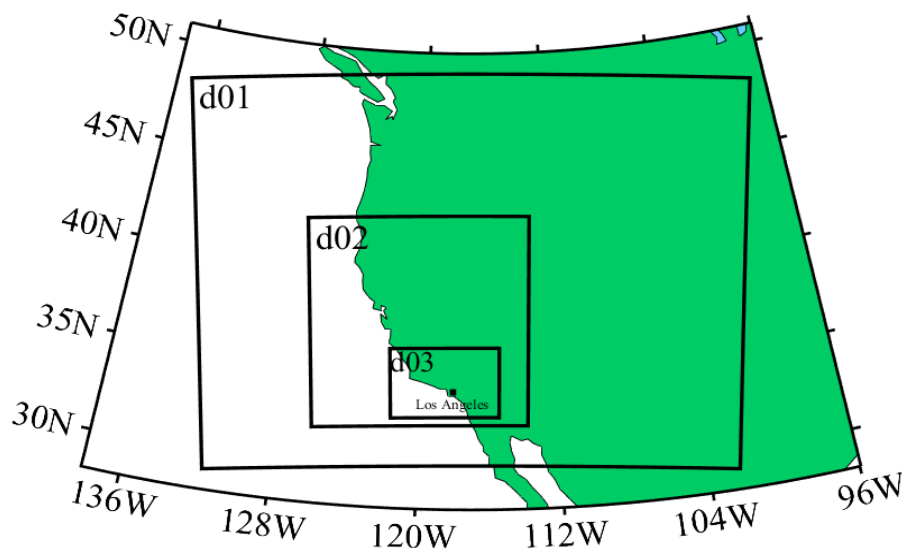
### 265 **3. WRF/Chem configuration and cross-correlations of emission species**

266 In this section, we describe the configuration of WRF/Chem, whose forecasting products will  
 267 be employed in the following BEC statistics and data assimilation experiments. In addition, the  
 268 cross-correlations of emission species from the WRF/Chem emission data are investigated to  
 269 understand the cross-correlation between different species of the BEC.

#### 270 **3.1 WRF/Chem configuration**

271 WRF/Chem (V3.5.1) is employed in our study. This is a fully coupled online model with a  
 272 regional meteorological model that is coupled to aerosol and chemistry models (Grell et al., 2005).  
 273 The model domain with three spatial domains is shown in Figure 1. The horizontal grid spacing  
 274 for these three domains are 36 km ( $80 \times 60$  points), 12 km ( $97 \times 97$  points), and 4 km ( $144 \times 96$   
 275 points), respectively. The outer domain spans southern California and the innermost domain

276 encompasses Los Angeles. All domains have 31 vertical levels with the top at 50 hPa. The vertical  
277 grid is stretched to place the highest resolution in the lower troposphere. The discussion of the  
278 BEC and the emissions presented in this paper will be confined to the innermost domain. The  
279 initial meteorology conditions for WRF/Chem are prepared using the North American Regional  
280 Reanalysis (NARR) (Mesinger et al. 2006). The meteorology boundary conditions and sea surface  
281 temperatures are updated at each initialization. For the forecast running, the initial meteorological  
282 conditions are obtained from the NARR data. The initial aerosol conditions are obtained from the  
283 former forecast. The emissions are derived from the National Emission Inventory 2005 (NEI'05)  
284 for both aerosols and trace gases (Guenther et al., 2006). For more details, the readers are referred  
285 to Li et al. (2013).



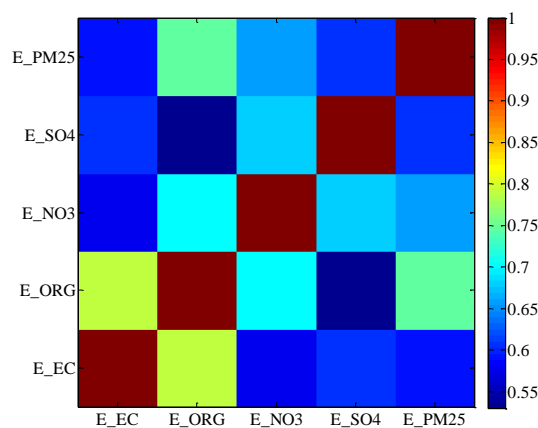
286  
287 Figure 1. Geographical display of the three-nested model domains. The innermost domain covers  
288 the Los Angeles basin; the black point denotes the location of Los Angeles.

### 289 3.2 Cross-correlations of emission species

290 The emission source is necessary for running the WRF/Chem model. It is an important factor  
291 for the distribution of the aerosol forecasts. The analysis of the correlations among the emission  
292 species can help us to understand the BEC statistics. The emission species is derived from the  
293 emission file that is produced by the NEI'05 data for each model domain. Only the emission data  
294 for the innermost domain is used to calculate the correlation among the emission species. The  
295 emission file contains 37 variables, including gas species and aerosol species. An aerosol species  
296 also comprises a nuclei mode and accumulation model species (Peckam et al., 2013). From these

297 aerosol emission species, five lumped aerosol species are calculated, which is consistent with the  
298 variables in the data assimilation. These five lumped species are E\_EC (sum of the nuclei mode  
299 and the accumulation mode of elemental carbon PM<sub>2.5</sub>), E\_ORG (sum of the nuclei mode and the  
300 accumulation mode of organic PM<sub>2.5</sub>), E\_NO3 (sum of the nuclei mode and the accumulation  
301 mode of nitrate PM<sub>2.5</sub>), E\_SO4 (sum of the nuclei mode and the accumulation mode of sulfate  
302 PM<sub>2.5</sub>), and E\_PM25 (sum of the nuclei mode and the accumulation mode of unspciated primary  
303 PM<sub>2.5</sub>).

304 Figure 2 shows the cross-correlations of the five lumped aerosol emission species. All  
305 cross-correlations exceed 0.5. This result reveals that the emission species are correlated, which  
306 may be attributed to the common emission sources and diffusion processes that are controlled by  
307 the same atmospheric circulation. The most significant cross-correlation is between E\_EC and  
308 E\_ORG with a value of approximately 0.8. This high correlation demonstrates that the emission  
309 distributions of these two species are very similar. Their emissions are primary in urban and  
310 suburban areas with small emissions in rural areas and along roadways (not shown). As shown in  
311 Fig. 2, the lowest cross-correlation is between E\_ORG and E\_SO4; the latter emissions are  
312 primary in the urban and suburban areas with few emissions in rural areas and roadways (not  
313 shown).



314  
315 Figure 2. Cross-correlations between emission species of E\_EC, E\_ORG, E\_NO3, E\_SO4 and  
316 E\_PM25. The emission species data are derived from the NEI'05 emissions set for the innermost  
317 domain of the WRF/Chem model

318

#### 319 4 Balance constraints and BEC statistics

320 With the configuration of the WRF/Chem model described in Section 3.1, forecasts for one  
321 month (from 00UTC of May 15 to 00UTC of June 14, 2010) were performed for the balance  
322 constraints and the BEC statistics. Forecast differences between 24 h forecasts and 48 h forecasts  
323 are available at 00UTC. Thirty forecast differences are employed as inputs in the NMC method.  
324 For this method, 30 forecast differences are sufficient; however, a longer time series may be more  
325 beneficial for the BEC statistics (Parrish and Derber, 1992).

#### 326 4.1 Balance regression statistics

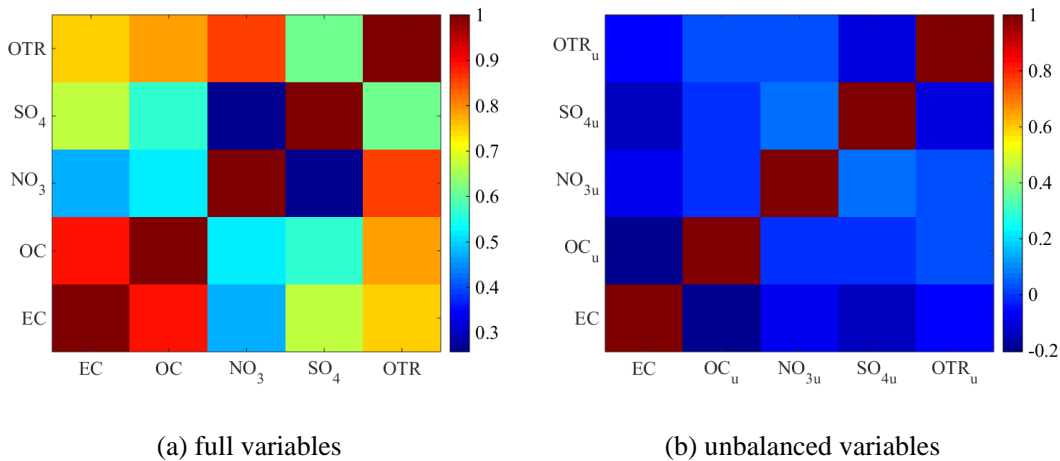
327 Using the 30 forecast differences between 24 h and 48 h forecasts, we can obtain  $\delta EC$ ,  $\delta OC$ ,  
328  $\delta NO_3$ ,  $\delta SO_4$  and  $\delta OTR$ . The size of these variables is  $(N \times 30)$ , where  $N$  is the number of  
329 model grid points. We put these data into Eqs. (6-13) to calculate the regression coefficients of  $\rho_{ij}$   
330 and the unbalanced parts of the variables. Note the process of calculation should be step by step,  
331 since the latter equation will use the unbalanced parts of former equations. Table 1 shows the  
332 regression coefficients whose column and row are consistent with  $\rho_{i,j}$  in Eq. (7). The last column  
333 in Tab. 1 is the coefficient of determination ( $R^2$ ) of the regression equations. For the regression  
334 equation of OC, the regression coefficient is 0.90 and the coefficient of determination of Eq. (7) is  
335 0.86, which indicates that EC and OC are highly correlated and their mass concentration scales are  
336 approximate. Their correlation is similar to the correlation of the stream function and velocity  
337 potential; thus, we set them as the first and second variables in the regression statistics. For the  
338 regression equation of  $NO_3$ , the regression coefficients of EC and  $OC_u$  are 4.01 and 3.76,  
339 respectively, because the mass concentration scale of  $NO_3$  exceeds the mass concentration scales  
340 of EC and  $OC_u$ . The coefficient of determination is only 0.32, which indicates that the  
341 correlations between  $NO_3$  and EC and between  $NO_3$  and  $OC_u$  are weak. This result reveals that  
342 the forecast errors of  $NO_3$  differ from the forecast errors of EC and  $OC_u$ . A possible reason is  
343 that  $NO_3$  is the secondary particle that is primarily derived from the transformation of  $NO_x$ , but  
344 EC and  $OC_u$  are derived from direct emissions. Similar to  $NO_3$ ,  $SO_4$  is also primarily derived  
345 from the transformation of  $SO_2$  and the coefficient of determination for  $SO_4$  is also low. For the  
346 last variable OTR, the maximum coefficient of determination is 0.96 because OTR includes some  
347 different compositions that are correlated with the first four variables.

348 Table 1 Regression coefficients of balance operator  $\mathbf{K}$  and the coefficient of determination  
 349 (regression coefficients correspond to  $\rho_{ij}$  in Eq. (7))

species	regression coefficient ( $\rho$ )					coefficient of determination ( $R^2$ )
EC	1					/
OC	0.90	1				0.86
NO <sub>3</sub>	4.01	3.76	1			0.32
SO <sub>4</sub>	1.35	-0.21	-3.15	1		0.48
OTR	2.93	2.35	0.28	0.60	1	0.96

350

351 Figure 3 shows the cross-correlations of the five full variables and the unbalanced variables. In  
 352 Fig. 3a, the cross-correlations of the full variables exceed 0.3 and most of them exceed 0.5. In Fig.  
 353 3b, however, the cross-correlations of the unbalanced variables are less than 0.2. Some of the  
 354 cross-correlations are close to zero, which indicates that these unbalanced variables are  
 355 approximatively independent and can be employed as control variables in the data assimilation  
 356 system.



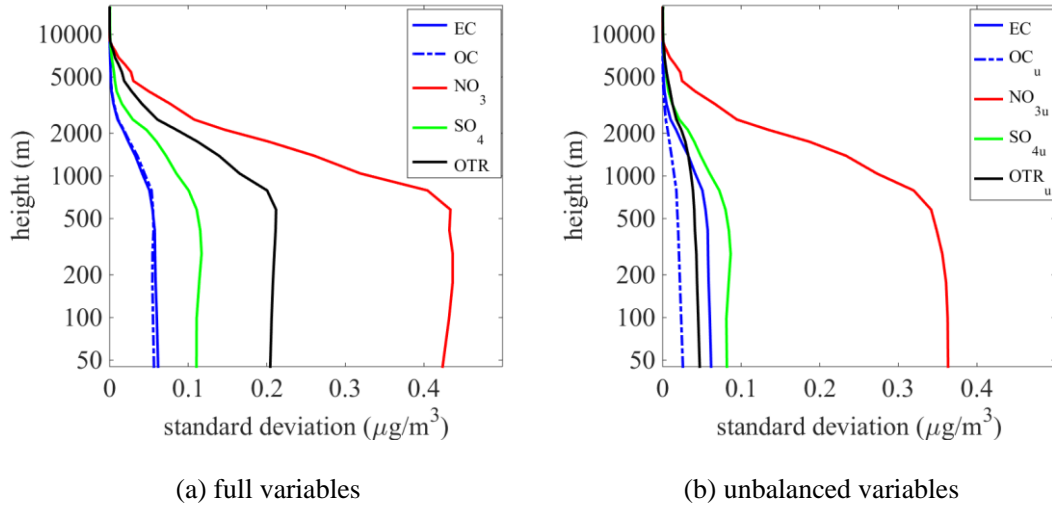
357 Figure 3. Cross-correlations between the five variables of the BEC. These variables are (a) full  
 358 variables and (b) unbalanced variables of EC, OC, NO<sub>3</sub>, SO<sub>4</sub> and OTR.

359

#### 360 4.2 BEC statistics

361 Using the original full variables and the unbalanced variables obtained by the regression  
 362 equations, the BEC statistics are **obtained**. Figure 4 shows the vertical profiles of the standard

363 deviations of the original  $\mathbf{D}$  and the unbalanced  $\mathbf{D}_u$ . In Fig. 4a, the original standard deviation of  
 364  $\text{NO}_3$  is the largest value, whereas the smallest value is OC, whose profile is close to the profile of  
 365 EC. All profiles show a significant decrease at approximately 800 m because the aerosol  
 366 particulates are usually limited under the boundary level. In Fig. 4b, all standard deviations  
 367 decrease in different degree, with the exception of EC, which remains as the control variable in the  
 368 unbalanced BEC statistics. Note that the standard deviation of  $\text{OTR}_u$  decreases by approximately  
 369 80% compared with  $\text{NO}_{3u}$ , which decreases by approximately 10%. This result is attributed to the  
 370 small coefficient of determination for the regression of  $\text{NO}_3$  (in Tab. 1), which indicates that a  
 371 small portion of  $\text{NO}_3$  can be predicted by the regression and a large portion is an unbalanced  
 372 component. In contrast with  $\text{NO}_3$ , a small portion of OTR is the unbalanced component.



373 Figure 4. Vertical profiles of the standard deviation of the variables. (a) full variables and (b)  
 374 unbalanced variables

375

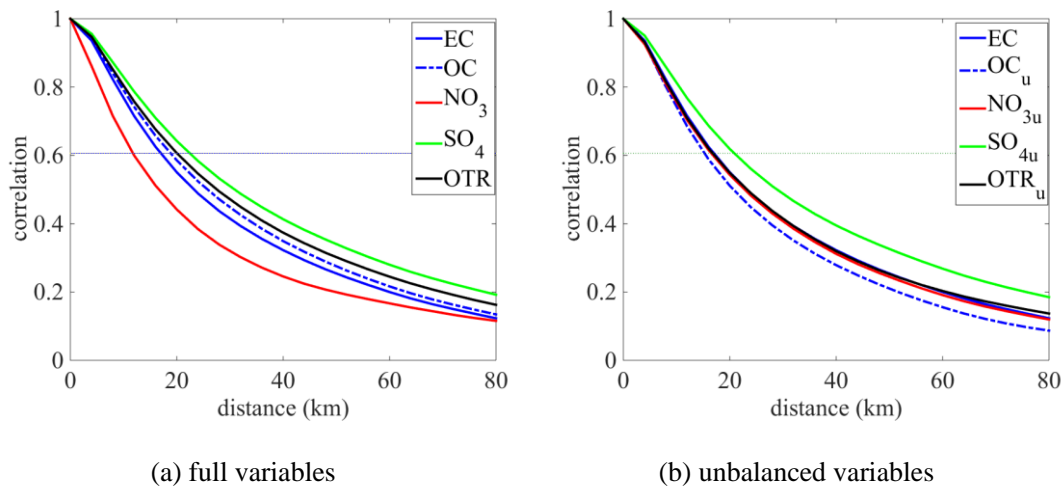
376 For the correlation matrix of  $\mathbf{C}$  and  $\mathbf{C}_u$ , they are factorized as three independent  
 377 one-dimensional correlation matrices in Eq. (24). The horizontal correlation  $\mathbf{C}_x$  or  $\mathbf{C}_y$  is  
 378 approximately expressed by a Gaussian function. The correlation between two points  $r_1$  and  $r_2$

379 can be written as  $e^{-\frac{(r_2-r_1)^2}{2L_s^2}}$ , where  $L_s$  is the horizontal correlation scale and is a constant value

380 for  $\mathbf{C}_x$  and  $\mathbf{C}_y$ , which are considered to be isotropic (Li et al., 2013). This scale can be estimated

381 by the curve of the horizontal correlations with distances. Figure 5 shows the curves of the

382 horizontal correlations for the five control variables. For the full variables (Fig. 5a), the sharpest  
 383 decrease in the curves is observed for  $\text{NO}_3$  and the slowest decrease in the curves is observed  
 384 for  $\text{SO}_4$ . We assume that the decline curve is according to the Gaussian function. Then the  
 385 intersection of the decline curve and the line of  $e^{-\frac{1}{2}}$  ( $\approx 0.61$ ) can be approximately as the value  
 386 of horizontal correlation scale. The horizontal correlation scales of EC, OC,  $\text{NO}_3$ ,  $\text{SO}_4$  and OTR  
 387 are 25 km, 27 km, 20 km, 30 km and 28 km, respectively. For the unbalanced variables (Fig. 5b),  
 388 their curves are closer than the curves of the full variables. The correlation scales of EC,  $\text{OC}_u$ ,  
 389  $\text{NO}_{3u}$ ,  $\text{SO}_{4u}$  and  $\text{OTR}_u$  are 25 km, 23 km, 24 km, 28 km and 25 km, respectively. These results  
 390 suggest that the unbalanced variables are expressed by some common factors such as EC,  $\text{OC}_u$   
 391 and  $\text{NO}_{3u}$ , in the regression equations of Eqs. (10-13), which produces consistent horizontal  
 392 correlation scales.

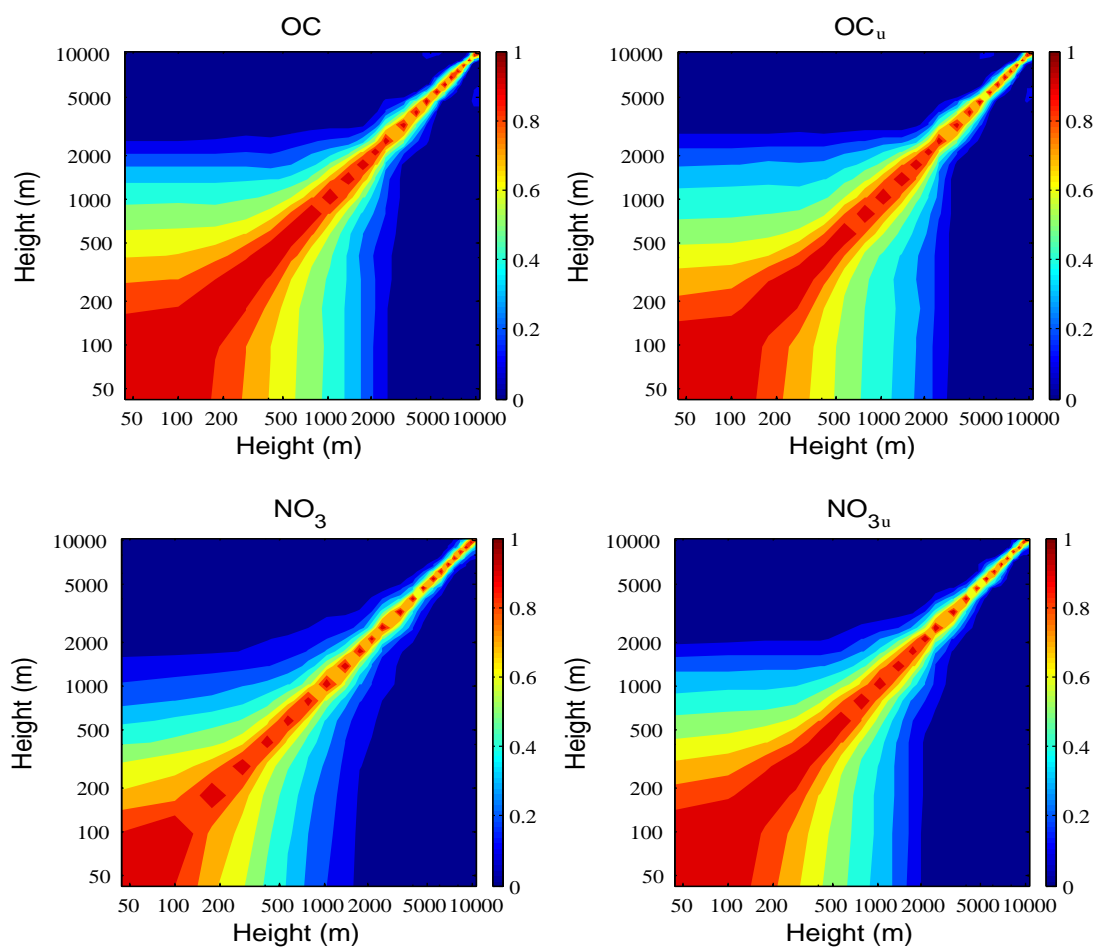


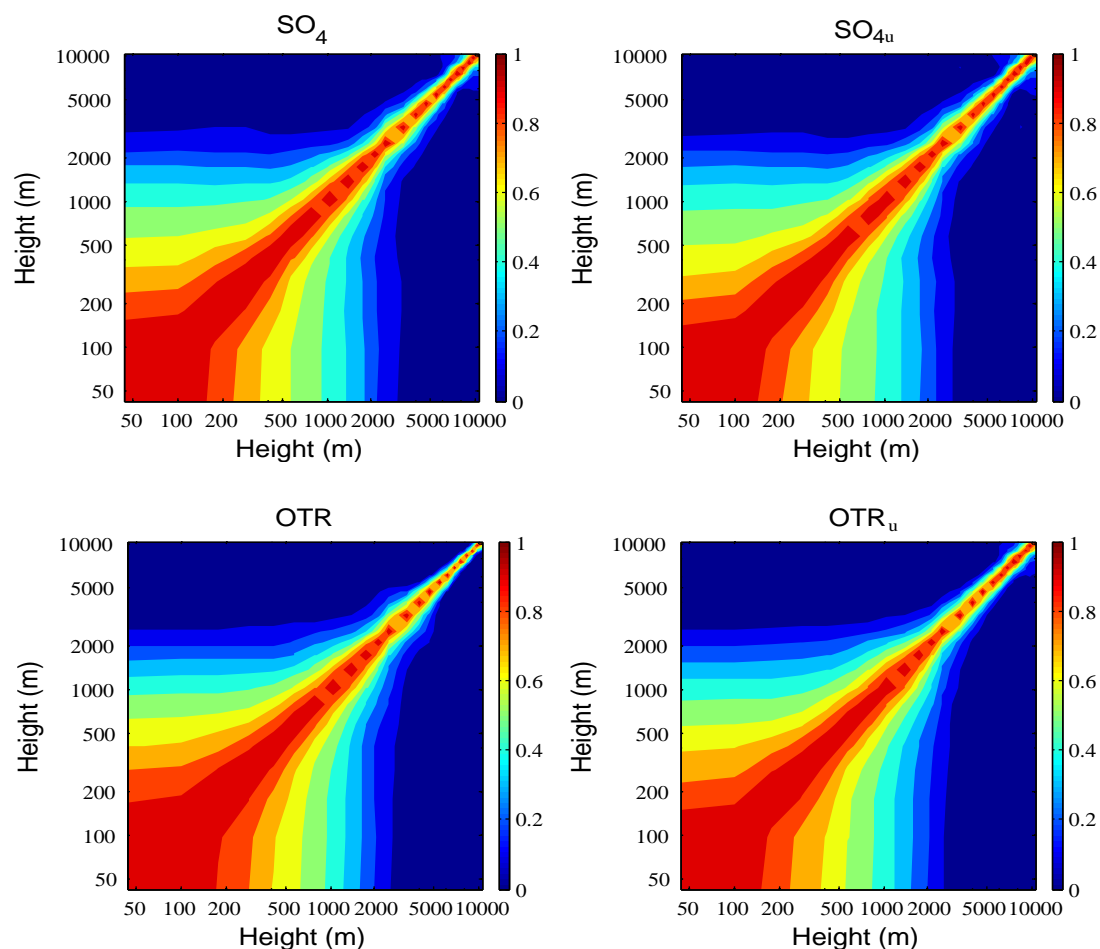
393 Figure 5. Same as Figure 4, with the exception of the horizontal auto-correlation curves of the  
 394 variables. The horizontal thin line is the reference line of  $e^{-\frac{1}{2}}$  ( $\approx 0.61$ ) for determining the  
 395 horizontal correlation scales.

396

397 For the vertical correlation between  $\mathbf{C}_z$  and  $\mathbf{C}_{uz}$ , they are directly estimated using the  
 398 forecasting differences in the data assimilation system, but not estimated from a approximately  
 399 alternative function. Because it is only an  $n_z \times n_z$  matrix. Figure 6 shows the vertical correlation  
 400 matrices  $\mathbf{C}_z$  and  $\mathbf{C}_{uz}$  for the full variables (left column) and the unbalanced variables (right  
 401 column), respectively. A common feature of both the full variables and the unbalanced variables is

402 the significant correlation between the levels of the boundary layer height, which is consistent  
403 with the profile of the standard deviation in Fig. 4. Some weak adjustments to the correlations  
404 between the full and unbalanced variables are made. For example, the correlation of  $\text{NO}_{3u}$  is  
405 stronger than the correlation of  $\text{NO}_3$  between the boundary layers. Similar with the analysis of  
406 horizontal correlation scale, the vertical correlation scale of  $\text{NO}_{3u}$  is larger than the vertical  
407 correlation scale of  $\text{NO}_3$ . Conversely, the vertical correlation scale of  $\text{OTR}_u$  is smaller than the  
408 vertical correlation scale of  $\text{OTR}$ . These results demonstrate that the vertical correlations for the  
409 unbalanced variables are more consistent than the vertical correlations of the full variables, which  
410 is similar to the adjustments to the horizontal correlation scale. Note that the differences of vertical  
411 correlation are slight, compared with the difference of horizontal. The main reason is that the  
412 vertical correlations are generally affected by the atmospheric boundary layer height. Thus, all  
413 vertical correlation decreases rapidly for the levels above the boundary layer height.





414 Figure 6. Vertical correlations of the five variables of the BEC. The left column represents the full  
 415 variables, and the right column represents the unbalanced variables.

416

## 417 5. Application to data assimilation and prediction

418 To exhibit the effect of the balance constraint of the BEC, the data assimilation experiments  
 419 and 24-h forecasts for nine cases are run using WRF/Chem model. The surface  $PM_{2.5}$  and  
 420 aircraft-speciated observations are assimilated using different BEC, and the evaluations are  
 421 presented for the data assimilation and subsequent forecasts. Three basic statistical measures  
 422 including mean bias (BIAS), root mean square error (RMSE) and correlation coefficient (CORR)  
 423 are utilized for the evaluations.

### 424 5.1 Observation data and experiment scheme

425 Two types of observation data are employed in our experiments. The first type of observation  
 426 data consists of hourly surface  $PM_{2.5}$  concentrations from the California Air Resources Board  
 427 (ARB). There are 42 surface  $PM_{2.5}$  monitoring sites existed in the innermost domain of the

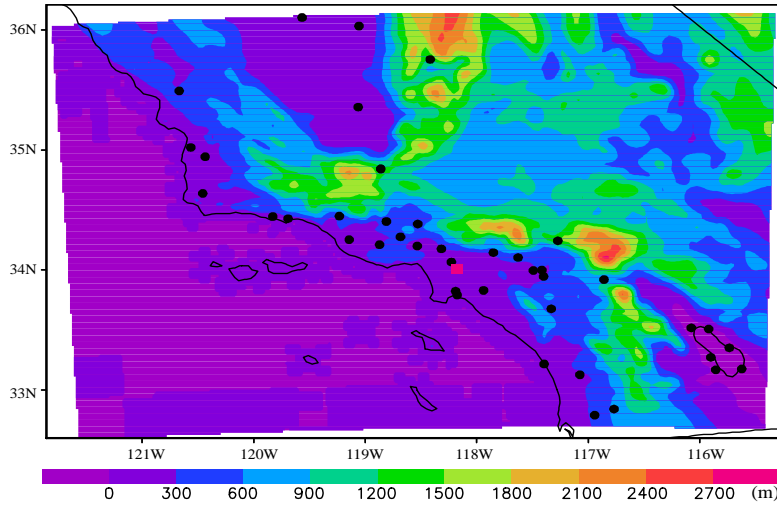
428 WRF/Chem model (Fig. 7). The second type of observation data is the speciated concentration  
 429 along the aircraft flight track. The aircraft observations were investigated from the California  
 430 Research at the Nexus of Air Quality and Climate Change (CalNex) field campaign in 2010. Nine  
 431 flights data around Los Angeles from 15 May to 14 June, 2010 are selected as the cases of data  
 432 assimilation. Table 2 shows the start time and end time of each flight. The species of the aircraft  
 433 observations include OC, NO<sub>3</sub>, SO<sub>4</sub> and NH<sub>4</sub>. Note that NH<sub>4</sub> is not a control variable; thus, the  
 434 aircraft observation of NH<sub>4</sub> is disregarded in the data assimilation. Because the particle size of the  
 435 aircraft observations is less than 1.0 μm, some adjustments to the flight observations are made  
 436 according to the ratios between the concentration under 2.5 μm and the concentration under 1.0  
 437 μm for each species using model products. With the ratios multiplied by the aircraft observed  
 438 concentrations, the speciated concentrations under 2.5 μm can be obtained.

439

440 **Table 2 The periods of flight during CalNex 2010 and the initial time of assimilation**

Number of cases	Start time of flight	End time of flight	Initial time of assimilation
1	18:00 UTC, May 16	01:42 UTC, May 17	00:00 UTC, May 17
2	17:28 UTC, May 19	00:10 UTC, May 20	18:00 UTC, May 19
3	17:28 UTC, May 21	00:10 UTC, May 21	18:00 UTC, May 21
4	23:08 UTC, May 24	05:23 UTC, May 25	00:00 UTC, May 25
5	01:59 UTC, May 30	07:45 UTC, May 30	06:00 UTC, May 30
6	05:00 UTC, May 31	10:54 UTC, May 31	06:00 UTC, May 31
7	07:59 UTC, June 2	14:09 UTC, June 2	12:00 UTC, June 2
8	07:59 UTC, June 3	14:04 UTC, June 3	12:00 UTC, June 3
9	17:56 UTC, June 14	23:35 UTC, June 14	18:00 UTC, June 14

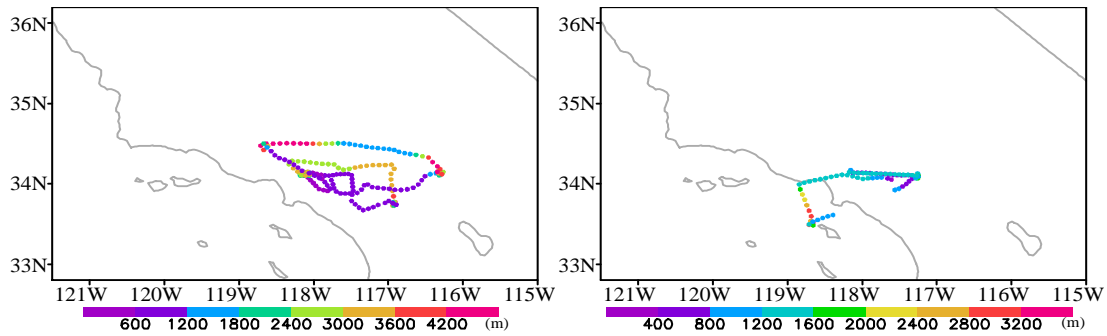
441



442

443 **Figure 7. The topography of the innermost domain and the locations of surface monitoring stations**  
 444 **(black dots). The red square is the location of Los Angeles**

445

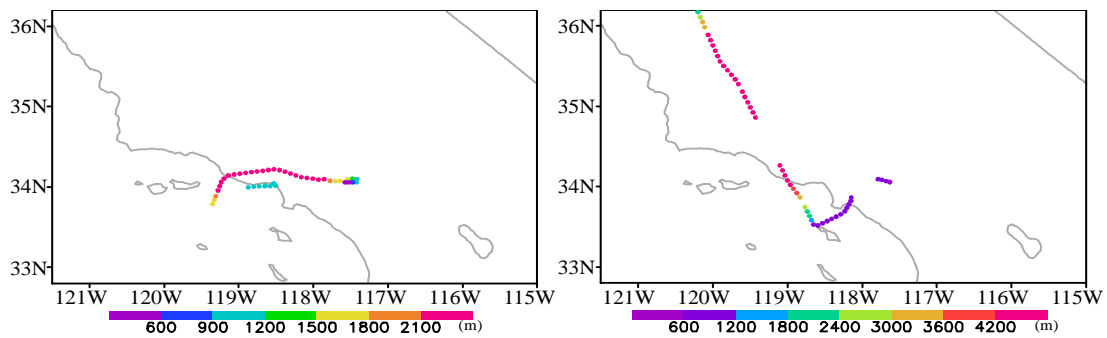


446

447

(a) 00:00 UTC ± 1.5 h, May 17

(b) 18:00 UTC ± 1.5 h, May 19

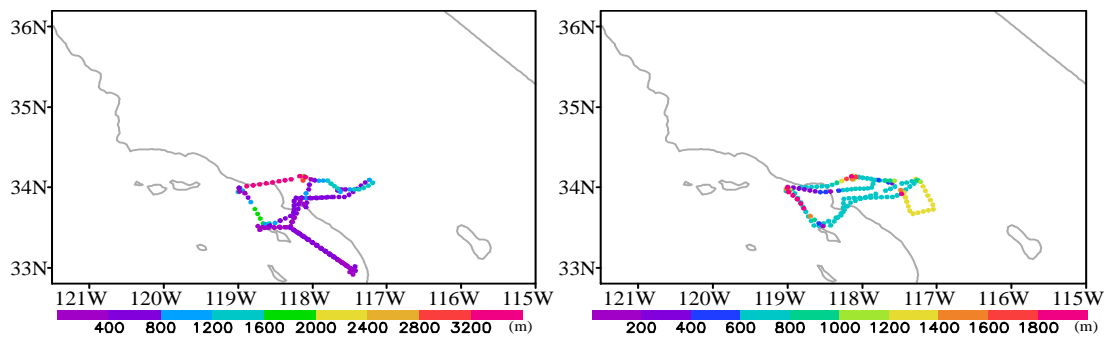


448

449

(c) 18:00 UTC ± 1.5 h, May 21

(d) 00:00 UTC ± 1.5 h, May 25

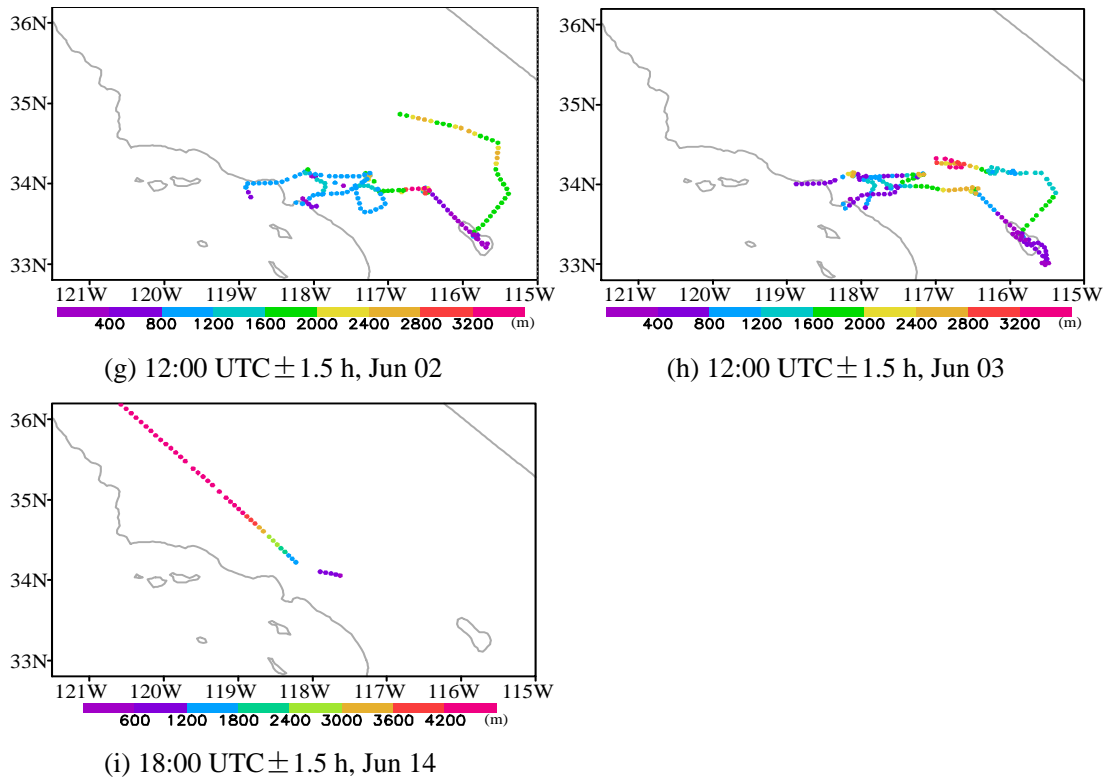


450

451

(e) 06:00 UTC ± 1.5 h, May 30

(f) 06:00 UTC ± 1.5 h, May 31



452  
453  
454  
455  
456 **Figure 8. Aircraft flight tracks during the time window of data assimilation for nine cases. The**  
457 **color of the track indicates the aircraft height.**

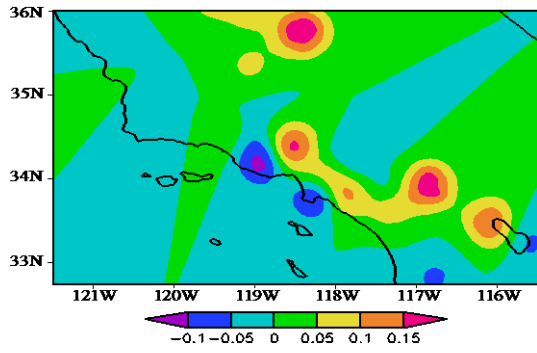
458  
459 **The initial time of data assimilation cases are designed according to the period of flights,**  
460 **showed in Table 2. The time window of assimilation for the flight data is  $\pm 1.5$ h, though some**  
461 **flight times do not completely cover the time windows. Figure 8 shows the aircraft tracks during**  
462 **the time window of data assimilation. It is obvious that the aircraft data on May 21, May 25 and**  
463 **June 14 are relative few as the tracks are almost outside of the study domain. For the surface data,**  
464 **it is only the observations at the initial time are assimilated. For each case, three parallel**  
465 **experiments are performed. The first experiment is the control experiment without aerosol data**  
466 **assimilation, which is frequently known as a free run and denoted as Control. The second**  
467 **experiment is a data assimilation experiment that assimilates surface  $PM_{2.5}$  and aircraft**  
468 **observations using the full variables without balance constraints; it is denoted as DA-full. The**  
469 **third experiment is also a data assimilation experiment that also assimilates surface  $PM_{2.5}$  and**  
470 **aircraft observations, but employs the unbalanced variables as control variables conducted by the**  
471 **balanced constraint; it is denoted as DA-balance. The backgrounds for DA-full and DA-balance**  
472 **are the forecasting results from the previous runs without DA. These previous forecasting results**

473 have been obtained when we run the model for the BEC statistics. The observation error is the half  
474 of standard deviation of the original background variable, and a vertical profile of observation  
475 errors is applied with the average profile of standard deviation of the background variable. In each  
476 experiment, a 24-h forecasting is run using the WRF/Chem model with the same configuration  
477 described in Section 3.1, and the case on June 3, 2010 is presented in detail as an example.

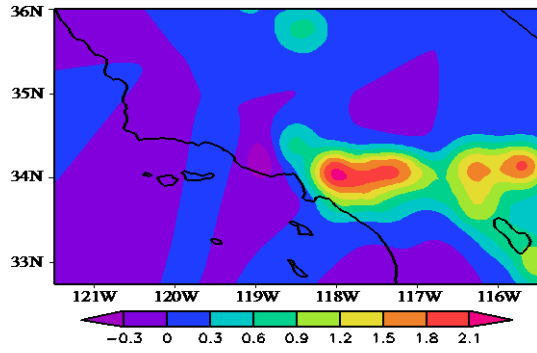
## 478 5.2 Increments of data assimilation

479 Figure 9 shows the horizontal increments of EC, OC, NO<sub>3</sub>, SO<sub>4</sub> and OTR at the first model  
480 level for the DA-full (left column) and DA-balance experiments (right column) of the case on  
481 June 3, 2010. In the DA-full experiment, the increment of EC and OTR (Fig. 9a and 9i) are similar.  
482 They are obtained from the surface PM<sub>2.5</sub> observations because no direct aircraft observations  
483 correspond to these two variables. In the DA-balance experiment, significant adjustments are  
484 made to the increments of EC (Fig. 9b) under the action of the balance constraints. The  
485 observations of OC affect greatly the increments of EC for thee high cross-correlation between EC  
486 and OC. Thus the increments of EC are similar with the increments of OC. Similarly, significant  
487 adjustments are made to the increment of OTR (Fig. 9j), though there are not the species  
488 observation of OTR. There are also some slight adjustments for the increments of OC, NO<sub>3</sub> and  
489 SO<sub>4</sub> for the crossing spread among species.

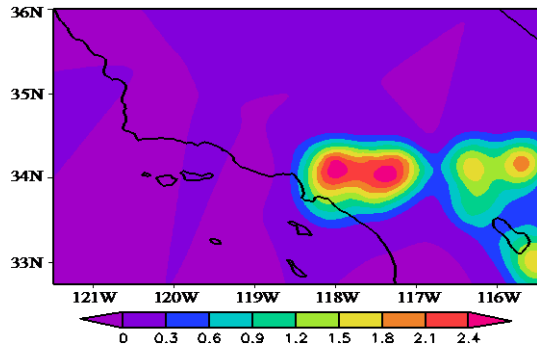
490 Figure 10 shows the vertical increments along 35.0 N for the DA-full and DA-balance  
491 experiments. Similar to Fig. 9, the increments of EC and OTR (Fig. 10a and 10i) spread upward  
492 from the surface in the DA-full experiment, which are obtained from the surface PM<sub>2.5</sub>  
493 observation. In the DA-balance, the increments of EC and OTR (Fig. 10b and 10j) exhibit  
494 observation information from the aircraft height at approximately 500 m, and the value of the  
495 increments show significant increases. The distributions of the increments for these five variables  
496 in the DA-balance (Fig. 10, right column) generally tend to coincide compared with the  
497 distributions of the increments in the DA-full (Fig. 10, left column). The results of the DA-balance  
498 are reasonable due to the influence of each other across the balance constraints.



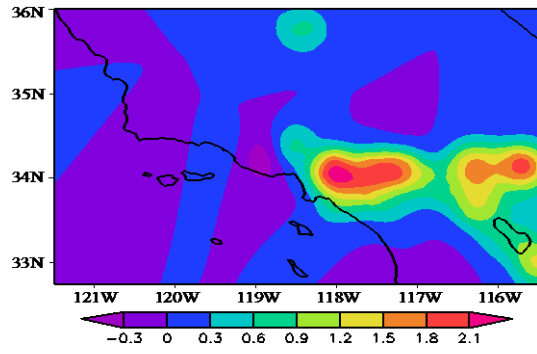
(a) EC in the DA-full



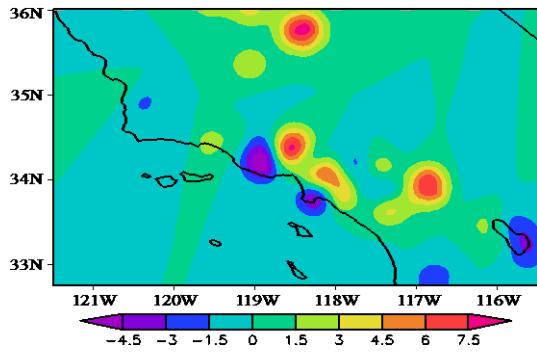
(b) EC in the DA-balance



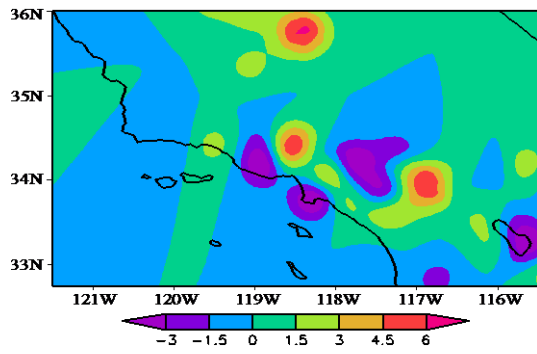
(c) OC in the DA-full



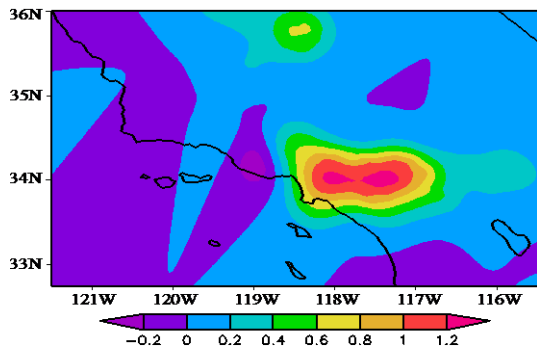
(d) OC in the DA-balance



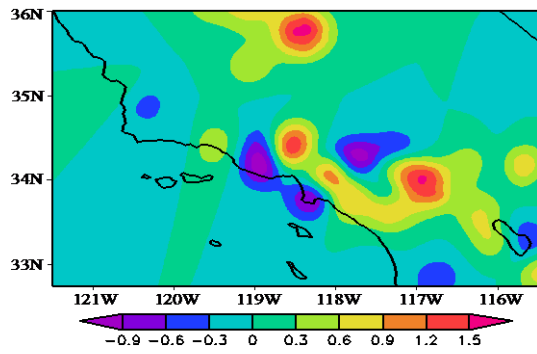
(e) NO<sub>3</sub> in the DA-full



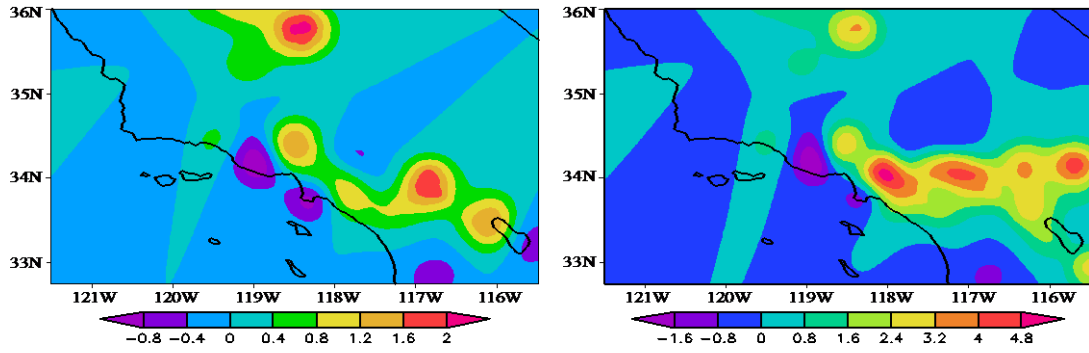
(f) NO<sub>3</sub> in the DA-balance



(g) SO<sub>4</sub> in the DA-full



(h) SO<sub>4</sub> in the DA-balance

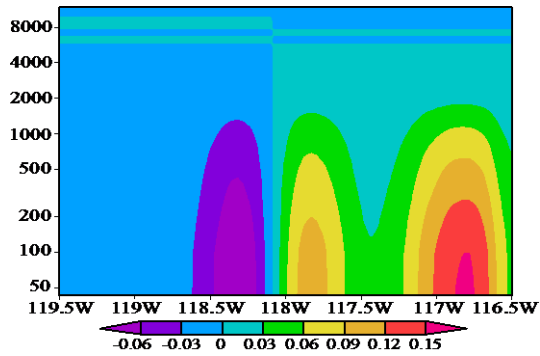


(i) OTR in the DA-full

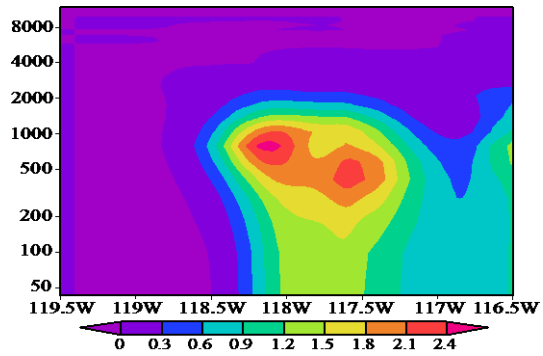
(j) OTR in the DA-balance

499 Figure 9. Surface distributions of increments of the five variables of EC, OC, NO<sub>3</sub>, SO<sub>4</sub> and OTR  
 500 at 12:00 UTC on June 3, 2010. The left column and right column are from DA-full and  
 501 DA-balance, respectively.

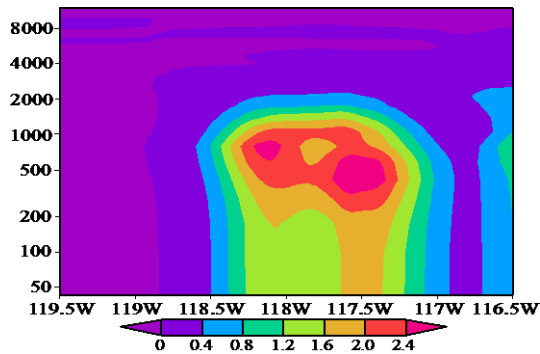
502



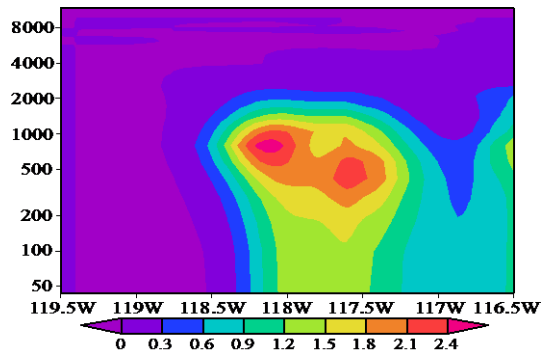
(a) EC in the DA-full



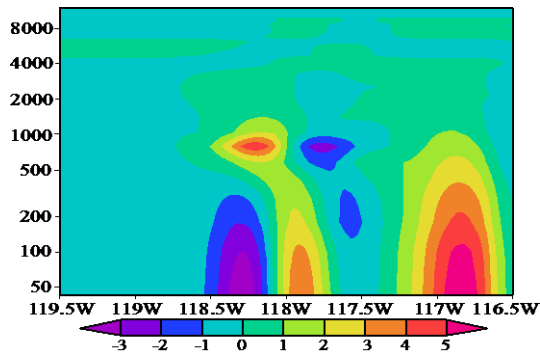
(b) EC in the DA-balance



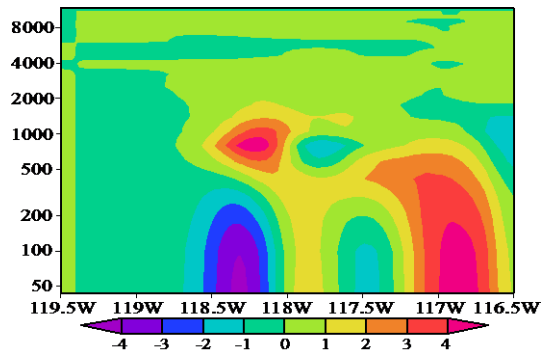
(c) OC in the DA-full



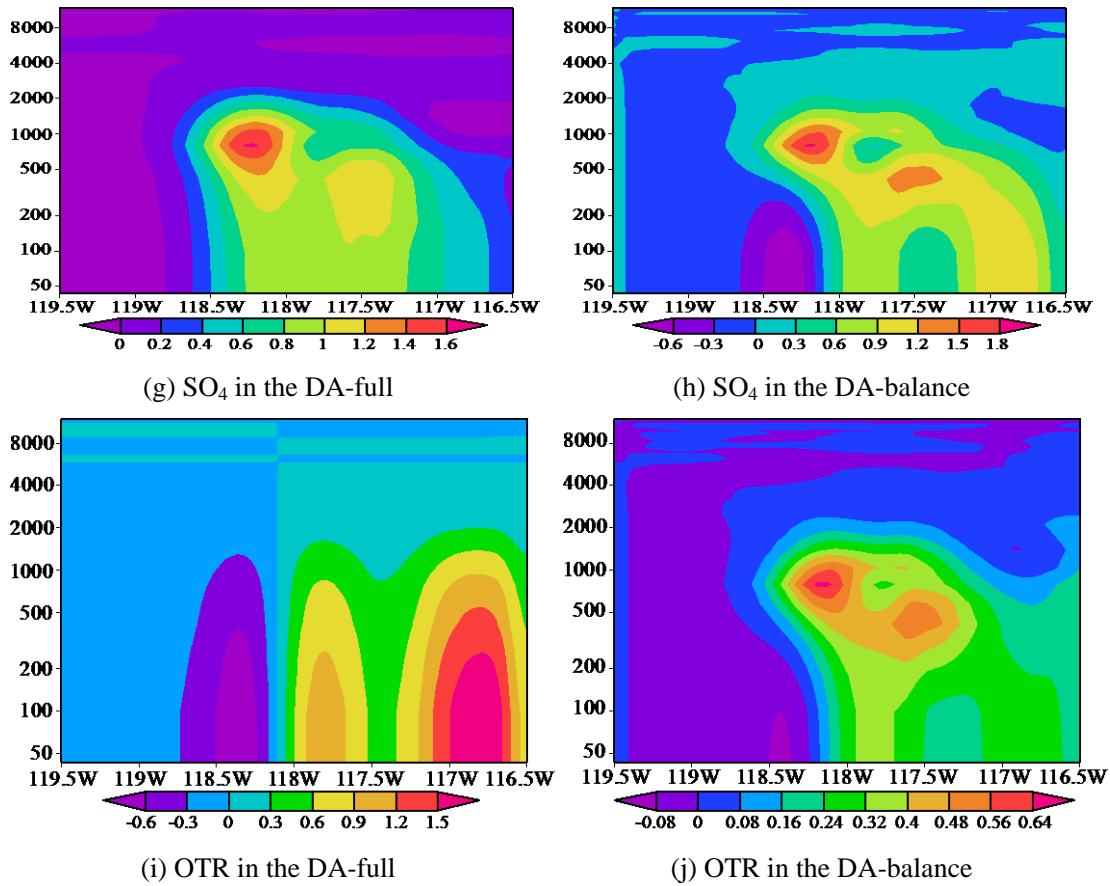
(d) OC in the DA-balance



(e) NO<sub>3</sub> in the DA-full



(f) NO<sub>3</sub> in the DA-balance

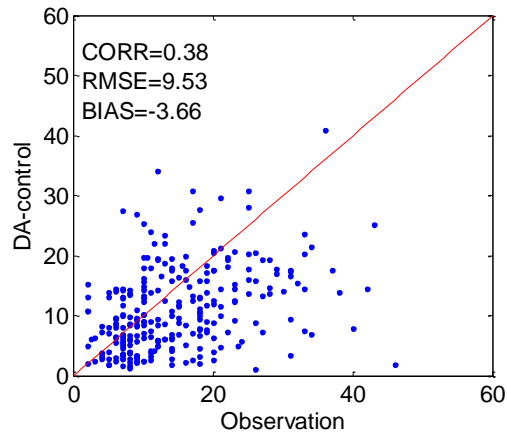


503 Figure 10. Same as Figure 9, with the exception of the vertical sections along 35 N.

504

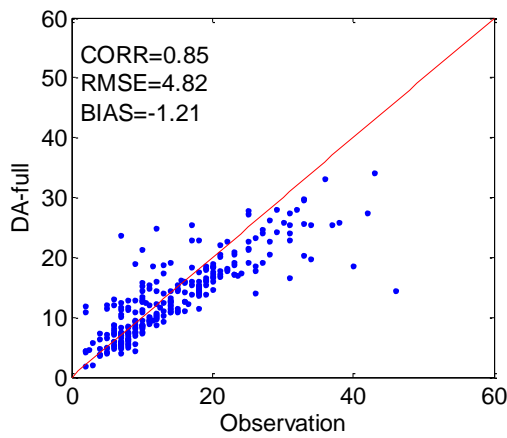
505 **5.3 Evaluation of data assimilation and forecasts**

506 Figure 11 shows the scatter plots of the initial model fields versus the surface observation for all  
 507 nine cases. In Fig. 11a, the simulated concentrations of the Control experiment display a  
 508 significant underestimation with a BIAS of  $-3.66 \mu\text{g}/\text{m}^3$ . The mean concentration of Control is  
 509  $10.90 \mu\text{g}/\text{m}^3$ , about 25.1% lower than observed mean concentrations ( $14.56 \mu\text{g}/\text{m}^3$ ). In the DA-full  
 510 and DA-balance experiments, there are remarkable increases for the simulated concentrations, and  
 511 the BIASs reduce to as small as  $-1.21$  and  $-0.94 \mu\text{g}/\text{m}^3$ . The RMSE is  $9.53 \mu\text{g}/\text{m}^3$  in the Control  
 512 experiment. The RMSE reduces to  $4.82$  and  $4.48 \mu\text{g}/\text{m}^3$  in the DA-full and DA-balance  
 513 experiment, respectively. There are also significant improvements for the CORR in the DA-full  
 514 and DA-balance experiments, compared with the Control experiment. Furthermore, these three  
 515 statistical measures of the DA-balance experiments show some slight improvement, compared  
 516 with that of the DA-full experiments. The result demonstrates that more observation information  
 517 spread by balance constraints can improve assimilation performance.



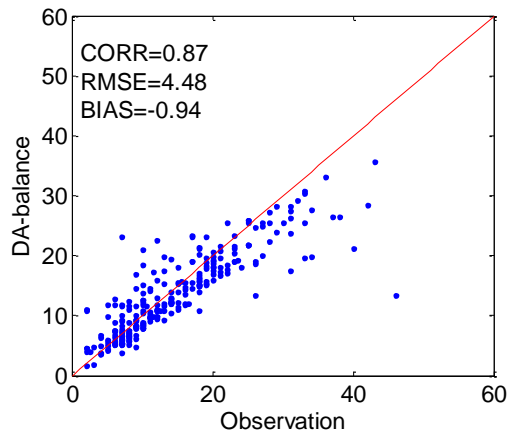
518  
519

(a) Control



520  
521

(b) DA-full



522  
523

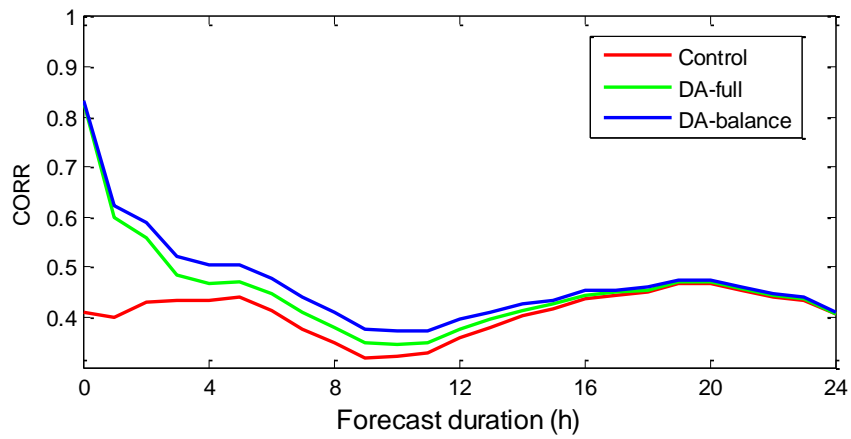
(c) DA-balance

524 Figure 11. Scatter plots of observed concentrations of  $PM_{2.5}$  versus simulated  $PM_{2.5}$  concentrations  
525 of the experiments of (a) Control, (b) DA-full, and (c) DA-balance for all nine cases.

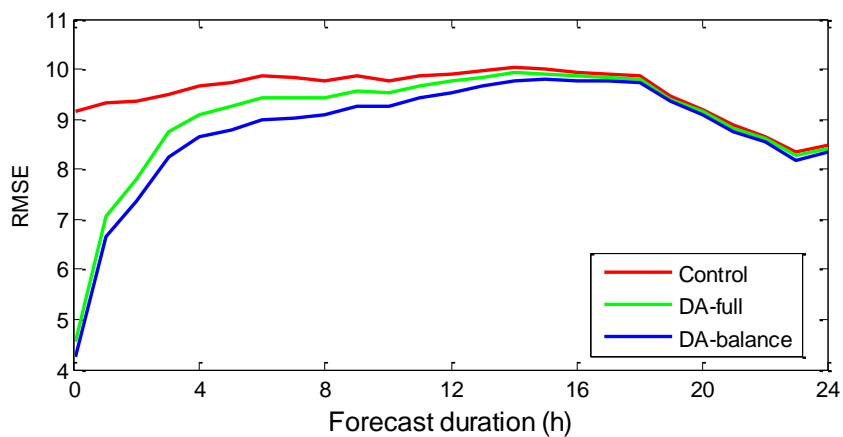
526

527 To evaluate the effects of the data assimilation, the CORR, RMSE and BIAS during the forecast  
528 time are calculated for each case, and their averaged results are showed in Figure 12. The CORRs  
529 of the DA-balance and DA-full experiments are very close (Fig. 12a). But, the difference increase

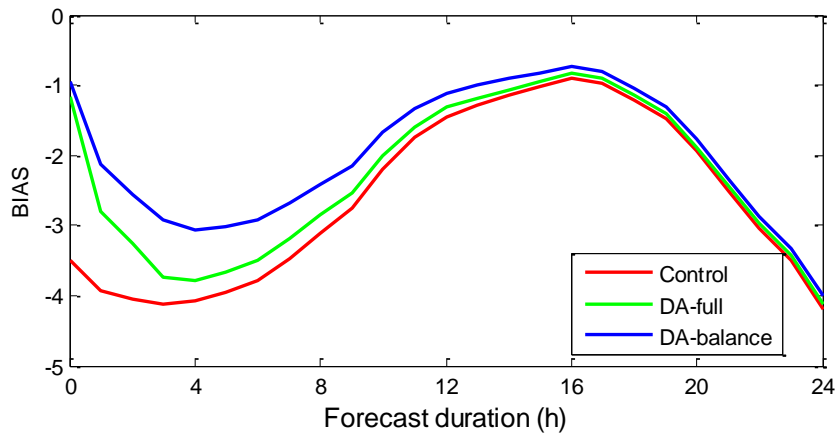
530 after the first hour with a higher CORR in the DA-balance experiment. The CORR of the  
531 DA-balance experiment is substantially higher than that of the DA-full experiment from the 2<sup>nd</sup>  
532 hour to the 16<sup>th</sup> hour. Similar improvements for the RMSE and the BIAS of the DA-balance  
533 experiment are observed in Fig. 12b and Fig. 12c, respectively. The improvement for the BIAS in  
534 the DA-balance experiment is the most significant among these three statistical measures. The  
535 peak value of the improvement for the BIAS (Fig 12c) is at the 4<sup>th</sup> hour, and the improvement is  
536 distinct until the end of forecasts. These improvements indicate that the balance constraint is  
537 positive for the subsequent forecasts, which derives from the balanced initial distribution among  
538 species.



(a) CORR



(b) RMSE



(c) BIAS

539 Figure 12. The averaged (a) Correlations, (b) root-mean-square errors (RMSE in  $\mu\text{g}/\text{m}^3$ ) and (c)  
 540 mean bias (BIAS in  $\mu\text{g}/\text{m}^3$ ) of the  $\text{PM}_{2.5}$  concentration forecasts against observations as a function  
 541 of forecast duration.

542

## 543 6. Summary and discussion

544 We examined the BEC in a 3DVAR system, which uses five control variables (EC, OC,  $\text{NO}_3$ ,  
 545  $\text{SO}_4$  and OTR) that are derived from the MOSAIC aerosol scheme in the WRF/Chem model.  
 546 Based on the NMC method, differences within a month-long period between 24- and 48-h  
 547 forecasts that are valid at the same time were employed in the estimation and analyses of the BEC.  
 548 The background errors of these five control variables are highly correlated. Especially between EC  
 549 and OC, their correlation is as large as 0.9.

550 A set of balance constraints was developed using a regression technique and incorporated in  
 551 the BEC to account for the large cross correlations. We employ the the balance constraint to  
 552 separate the original full variables into balanced and unbalanced parts. The regression technique is  
 553 used to express the balanced parts by the unbalanced parts. These unbalanced parts can be  
 554 assumed independent. Then, the unbalanced parts are employed as control variables in the BEC  
 555 statics. Accordingly, the standard deviations of these unbalanced variables are less than the  
 556 standard deviations of the original variables. The horizontal correlation scales of unbalanced  
 557 variables are closer than that of full variables on the effect of the balance constraints. And the  
 558 vertical correlations of unbalanced variables show similar trend.

559 To evaluate the impact of the balance constraints on the analyses and forecasts, three groups of  
 560 experiments, including a control experiment without data assimilation and two data assimilation

561 experiments with and without balance constraints (DA-full and DA-balance), were performed. In  
562 the data assimilation experiments, the observations of surface  $\text{PM}_{2.5}$  concentration and  
563 aircraft-speciated concentration of OC,  $\text{NO}_3$  and  $\text{SO}_4$  were assimilated. The observations of these  
564 three variables can spread to the two remaining variables in the increments of the DA-balance,  
565 which results in a more complex distribution. The evaluations of CORR, RMSE and BIAS for the  
566 initial analysis fields show more improvement in the DA-balance experiments, compared with the  
567 DA-full experiments. Though, these improvement are some slight. An important reason is that the  
568 surface  $\text{PM}_{2.5}$  observations are independent from the aircraft observations. If we evaluate the  
569 analysis fields by the species observation of aircraft, there may be more significant improvements  
570 in the DA-balance experiments.

571 While the improvements increase after the first forecasting hour in the DA-balance  
572 experiments, compared with forecasts of the DA-full experiments. The improvements persist to  
573 the end of forecasts, and are substantial from the 2<sup>nd</sup> hour to the 16<sup>th</sup> hour (Fig. 12). These results  
574 suggested that the balance constraints can serve an import role for continually improving the skill  
575 of sequent forecasts. Note that some aircraft data are relative few, and some flight tracks are not  
576 around Los Angeles in some cases (Fig. 8). If there are more aircraft observations, the  
577 improvements of the DA-balance experiments should be more significant and durable.

578 The developed method for incorporating balance constraints in aerosol data assimilation can  
579 be employed in other areas or other applications for different aerosol models. For the aerosol  
580 variables in different models, some cross-correlations between different species or size bins  
581 should exist because their common emissions and diffusion processes are controlled by the same  
582 atmospheric circulation. Although these cross-correlations may be stronger than the  
583 cross-correlations of atmospheric or oceanic model variables, theoretic balance constraints, such  
584 as geostrophic balance or temperature-salinity balance, do not exist. We expected to discover a  
585 universal balance constraint that can describe the physical or chemical balanced relationship of  
586 aerosol variables, and utilize it in the data assimilation system. In addition, we expected to expand  
587 the balance constraint to include gaseous pollutants, such as nitrite ( $\text{NO}_2$ ), sulfur dioxide ( $\text{SO}_2$ ),  
588 and (carbon monoxide) CO. These gaseous pollutants are correlated with some aerosol species,  
589 such as  $\text{NO}_3$ ,  $\text{SO}_4$  and EC, which can improve the data assimilation analysis fields of aerosols by

590 assimilating these gaseous observations. The assimilation of aerosol observations may improve the  
591 analysis fields of gaseous pollutants.

592

### 593 **Code availability**

594 This data assimilation system is established by ourself. The code of this system can be obtained on  
595 request from the first author ([zzlqxy@163.com](mailto:zzlqxy@163.com)).

596

### 597 **Acknowledgements**

598 This research was supported by the National Natural Science Foundation of China (41275128).

599 We gratefully thank the California Air Resources Board (<http://www.arb.ca.gov/homepage.htm>)

600 and NOAA Earth System Research Laboratory Chemical Sciences Division

601 (<http://esrl.noaa.gov/csd/groups/csd7/measurements/2010calnex/>), for providing the download of

602 surface and aircraft aerosol observations.

603

### 604 **References**

605 Bannister, R.N., 2008a. A review of forecast error covariance statistics in atmospheric variational  
606 data assimilation. I: Characteristics and measurements of forecast error covariances. *Quart. J. Roy.  
607 Meteor. Soc.*, 134, 1951–1970.

608 Bannister, R.N., 2008b. A review of forecast error covariance statistics in atmospheric variational  
609 data assimilation. II: Modelling the forecast error covariance statistics. *Quart. J. Roy. Meteor. Soc.*,  
610 134, 1971–1996.

611 Barker, D.M., Huang, W., Guo, Y.R., Xiao, Q.N., 2004. A Three-Dimensional (3DVAR) data  
612 assimilation system for use with MM5: implementation and initial results. *Mon. Weather Rev.* 132,  
613 897–914.

614 Benedetti, A., Fisher, M., 2007. Background error statistics for aerosols. *Quart. J. Roy. Meteor.  
615 Soc.*, 133, 391–405.

616 Chen, Y., Rizvi, S., Huang, X., Min, J., Zhang, X., 2013. Balance characteristics of multivariate  
617 background error covariances and their impact on analyses and forecasts in tropical and Arctic  
618 regions. *Meteorol. Atmos. Phys.*, 121, 79–98.

619 Cohn, S.E., 1997: Estimation theory for data assimilation problems: Basic conceptual framework

620 and some open questions. *J. Meteorol. Soc. Jpn.*, 75, 257–288.

621 Derber, J., Bouttier, F., 1999. A reformulation of the background error covariance in the ECMWF  
622 global data assimilation system. *Tellus*, 51, 195–221.

623 Geller, M. D., Fine, P. M., and Sioutas, C., 2004. The relationship between real-time and  
624 time-integrated coarse (2.5–10m), intermodal (1–2.5m), and fine (<2.5m) particulate matter in the  
625 Los Angeles basin. *Journal of the Air & Waste Management Association*, 54(9), 1029–1039.

626 Grell, G.A., Peckham, S.E., Schmitz, R., McKeen, S.A., Frost, G., Skamarock, W.C., Eder, B.,  
627 2005. Fully coupled “online” chemistry within the WRF model. *Atmos. Environ.*, 39, 6957–6976,  
628 doi:10.1016/j.atmosenv.2005.04.027.

629 Guenther, A., Karl, T., Harley, P., Wiedinmyer, C., Palmer, P.I., Geron, C., 2006. Estimates of  
630 global terrestrial isoprene emissions using MEGAN (Model of Emissions of Gases and Aerosols  
631 from Nature). *Atmos. Chem. Phys.*, 6, 3181–3210, doi:10.5194/acp-6-3181-2006.

632 Huang, X.Y., Xiao, Q., Barker, D.M., Zhang, X., Michalakes, J., Huang, W., Henderson, T., 2009.  
633 Four-dimensional variational data assimilation for WRF: formulation and preliminary results.  
634 *Mon. Weather Rev.*, 137, 299–314.

635 Jazwinski, A. H., 1970. *Stochastic processes and filtering theory*, Academic Press, New York, 376  
636 pp.

637 Kahnert, M., 2008. Variational data analysis of aerosol species in a regional CTM: background  
638 error covariance constraint and aerosol optical observation operators. *Tellus B*, 60(5), 753–770.

639 Li, Z., Zang, Z., Li, Q.B., Chao, Y., Chen, D., Ye, Z., Liu, Y., Liou, K.N., 2013. A  
640 three-dimensional variational data assimilation system for multiple aerosol species with  
641 WRF/Chem and an application to PM<sub>2.5</sub> prediction. *Atmos. Chem. Phys.*, 13, 4265–4278.

642 Liu, Z., Liu, Q., Lin, H.C., Schwartz, C.S., Lee, Y.H., Wang, T., 2011. Three-dimensional  
643 variational assimilation of MODIS aerosol optical depth: Implementation and application to a dust  
644 storm over East Asia. *J. Geophys. Res.*, 116, D23206, doi:10.1029/2011JD016159.

645 Mesinger, F., DiMego, G., Kalnay, E., Shafran, P., Ebisuzaki, W., Jovic, D., Woollen, J., Mitchell,  
646 K., Rogers, E., Ek, M., Fan, Y., Grumbine, R., Higgins, W., Li, H., Lin, Y., Manikin, G., Parrish,  
647 D., Shi, W., 2006. North American Regional Reanalysis. *B. Am. Meteorol. Soc.*, 87, 343–360.

648 Peckam, S.E., Grell, G.A., McKeen, S.A., Ahmadov, R., 2013. *WRF/Chem Version 3.5 User's*  
649 *Guide*. Colorado: NOAA Earth System Research Laboratory.

650 Pagowski, M., Grell, G. A., 2012. Experiments with the assimilation of fine aerosols using an  
651 ensemble Kalman filter, *J. Geophys. Res.*, 117, D21302, doi:10.1029/2012JD018333.

652 Pagowski, M., Grell, G.A., McKeen, S.A., Peckham, S.E., Devenyi, D., 2010. Three-dimensional  
653 variational data assimilation of ozone and fine particulate matter observations: Some results using  
654 the Weather Research and Forecasting–Chemistry model and Grid-point Statistical Interpolation.  
655 *Q. J. Roy. Meteorol. Soc.*, 136, 2013–2024, doi:10.1002/qj.700.

656 Parrish, D.F., Derber, J.C., 1992. The national meteorological center spectral statistical  
657 interpolation analysis. *Mon. Weather Rev.*, 120, 1747–1763.

658 Ricci, S., Weaver, A.T., 2005. Incorporating State-Dependent Temperature–Salinity Constraints in  
659 the Background Error Covariance of Variational Ocean Data Assimilation. *Mon. Weather Rev.*,  
660 133, 317–338.

661 Saide, P.E., Carmichael, G.R., Spak, S.N., Minnis, P., Ayers, J.K., 2012. Improving aerosol  
662 distributions below clouds by assimilating satellite-retrieved cloud droplet number. *P. Natl. Acad.*  
663 *Sci. USA*, 109, 11939–11943, doi:10.1073/pnas.1205877109.

664 Saide, P.E., Carmichael, G.R., Liu, Z., Schwartz, C.S., Lin, H.C., Da Silva, A.M., Hyer, E., 2013.  
665 Aerosol optical depth assimilation for a size-resolved sectional model: impacts of observationally  
666 constrained, multi-wavelength and fine mode retrievals on regional scale forecasts. *Atmos. Chem.*  
667 *Phys.*, 13, 10425–10444, doi:10.5194/acp-13-10425-2013.

668 Salako, G.O., Hopke, P.K., Cohen, D.D., Begum, B.A., Biswas, S.K., Pandit, G.G., Chung, Y.S.,  
669 Rahman, S.A., Hamzah, M.S., Davy, P., Markwitz, A., Shagjjamba, D., Lodoysamba, S.,  
670 Wimolwattanapun, W., Bunprapob, S., 2012. Exploring the Variation between EC and BC in a  
671 Variety of Locations. *Aerosol Air Qual. Res.*, 12, 1–7.

672 Wu, W.S., Purser, R.J., Parrish, D.F., 2002. Three-dimensional variational analysis with spatially  
673 inhomogeneous covariances. *Mon. Wea. Rev.*, 130, 2905-2916

674 Schwartz, C.S., Liu, Z., Lin, H.-C., McKeen, S.A., 2012. Simultaneous three-dimensional  
675 variational assimilation of surface fine particulate matter and MODIS aerosol optical depth. *J.*  
676 *Geophys. Res.*, 117, D13202, doi:10.1029/2011JD017383.

677 Schwartz, C. S., Liu, Z., Lin, H.-C., Cetola, J. D., 2014, Assimilating aerosol observations with a  
678 “hybrid” variational-ensemble data assimilation system, *J. Geophys. Res. Atmos.*, 119, 4043–4069,  
679 doi:10.1002/ 2013JD020937.

680 Sun C.-H., Lin Y.-C., Wang C.-S., 2003. 7. Relationships among Particle Fractions of Urban and  
681 Non-urban Aerosols. *Aerosol and Air Quality Research*, 3(1), 7-15.

682 Zaveri, R.A., Easter, R.C., Fast, J.D., Peters. L K., 2008. Model for Simulating Aerosol  
683 Interactions and Chemistry(MOSAIC). *J. Geophys. Res.*, 113, D13204,  
684 doi:10.1029/2007JD008782.

685

686

687

688

689

690

691

692

693

694

695

696

697

698

699

700

701

702

703

704

705

706

707

708

709

710

711 Table 1 Regression coefficients of balance operator  $K$  and the coefficient of determination712 (regression coefficients correspond to  $\rho_{ij}$  in Eq. (7))

species	regression coefficient ( $\rho$ )					coefficient of determination ( $R^2$ )
EC	1					/
OC	0.90	1				0.86
NO <sub>3</sub>	4.01	3.76	1			0.32
SO <sub>4</sub>	1.35	-0.21	-3.15	1		0.48
OTR	2.93	2.35	0.28	0.60	1	0.96

713

714

715

716

717 Table 2 The periods of flight during CalNex 2010 and the initial time of assimilation

Number of cases	Start time of flight	End time of flight	Initial time of assimilation
1	18:00 UTC, May 16	01:42 UTC, May 17	00:00 UTC, May 17
2	17:28 UTC, May 19	00:10 UTC, May 20	18:00 UTC, May 19
3	17:28 UTC, May 21	00:10 UTC, May 21	18:00 UTC, May 21
4	23:08 UTC, May 24	05:23 UTC, May 25	00:00 UTC, May 25
5	01:59 UTC, May 30	07:45 UTC, May 30	06:00 UTC, May 30
6	05:00 UTC, May 31	10:54 UTC, May 31	06:00 UTC, May 31
7	07:59 UTC, June 2	14:09 UTC, June 2	12:00 UTC, June 2
8	07:59 UTC, June 3	14:041 UTC, June 3	12:00 UTC, June 3
9	17:56 UTC, June 14	23:35 UTC, June 14	18:00 UTC, June 14

718

719

720

721

722

723 Figure 1 Geographical display of the three-nested model domains. The innermost domain covers  
724 the Los Angeles basin; the black point denotes the location of Los Angeles.

725

726 Figure 2 Cross-correlations between emission species of E\_EC, E\_ORG, E\_NO3, E\_SO4 and  
727 E\_PM25. The emission species data are derived from the NEI'05 emissions set for the innermost  
728 domain of the WRF/Chem model

729

730 Figure 3 Cross-correlations between the five variables of the BEC. These variables are (a) full  
731 variables and (b) unbalanced variables of EC, OC, NO<sub>3</sub>, SO<sub>4</sub> and OTR.

732

733 Figure 4 Vertical profiles of the standard deviation of the variables. (a) full variables and (b)  
734 unbalanced variables

735

736 Figure 5 Same as Figure 4, with the exception of the horizontal auto-correlation curves of the  
737 variables. The horizontal thin line is the reference line of  $e^{-\frac{1}{2}}$  ( $\approx 0.61$ ) for determining the  
738 horizontal correlation scales.

739

740

741 Figure 6 Vertical correlations of the five variables of the BEC. The left column represents the full  
742 variables, and the right column represents the unbalanced variables.

743

744 Figure 7 The topography of the innermost domain and the locations of surface monitoring stations  
745 (black dots). The red square is the location of Los Angeles

746

747 Figure 8 Aircraft flight tracks during the time window of data assimilation for nine cases. The  
748 color of the track indicates the aircraft height.

749

750 Figure 9 Surface distributions of increments of the five variables of EC, OC, NO<sub>3</sub>, SO<sub>4</sub> and OTR  
751 at 12:00 UTC on June 3, 2010. The left column and right column are from DA-full and  
752 DA-balance, respectively.

753

754 Figure 10 Same as Figure 9, with the exception of the vertical sections along 35 N.

755

756 Figure 11 Scatter plots of observed concentrations of  $PM_{2.5}$  versus simulated  $PM_{2.5}$  concentrations  
757 of the experiments of (a) Control, (b) DA-full, and (c) DA-balance for all nine cases.

758

759 Figure 12 The averaged (a) Correlations, (b) root-mean-square errors (RMSE in  $\mu\text{g}/\text{m}^3$ ) and (c)  
760 mean bias (BIAS in  $\mu\text{g}/\text{m}^3$ ) of the  $PM_{2.5}$  concentration forecasts against observations as a function  
761 of forecast duration.

762